CHAPTER 2

2. REVIEW OF THE RAIL TRACK SUBSTRUCTURE

2.1 Introduction

Conventional railway track substructure is a layered system; its components include ballast, sub-ballast, and subgrade soil providing support to the rail and sleepers (Fig. 2.1). In some literature the ballast and sub-ballast layers are defined as a combined "track support" layer. It could be observed from Fig. 2.1 that not all substructure systems include capping layers. Capping layer is provided to protect the natural ground or fill from moisture ingress and to form a unified subgrade layer.

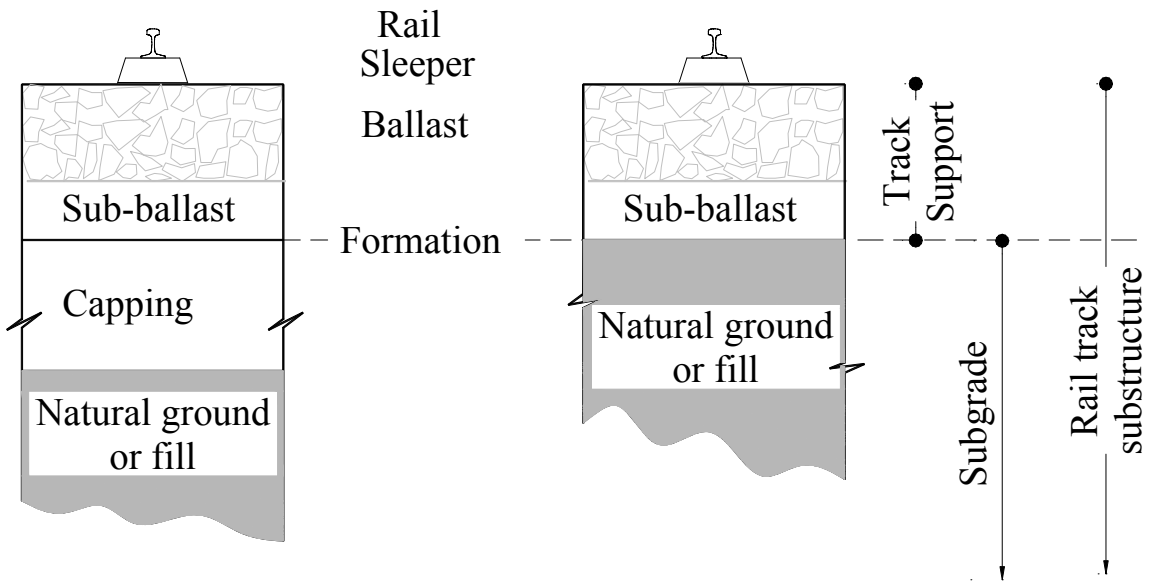

a) with capping layer b) without capping layer

Note:
Except for new construction, the boundaries between strata, as defined, may not be distinct.

Figure 2.1 Types and components of track substructure

Ballast or the track support layer keeps the rail and sleepers intact at the required position by resisting and dissipating the vertical, transverse and longitudinal forces transmitted by

the sleepers. It distributes the loads to the layers below, protecting the subgrade from high stresses and attenuates the noise and shock in addition to providing immediate drainage. The ideal ballast must be of uniform quality, preferably angular in shape with hard corners, usually with all dimensions nearly equal, and clean and free from dust and other contaminants. An appropriate thickness of the ballast layer helps in preventing track buckling.

Fig. 2.2 illustrates the Particle sizes for ballast specified by Queensland Rail (QR); at least 80% by weight of particles forming ballast shall be of crushed rocks (Specification No CT147 2001, QR).

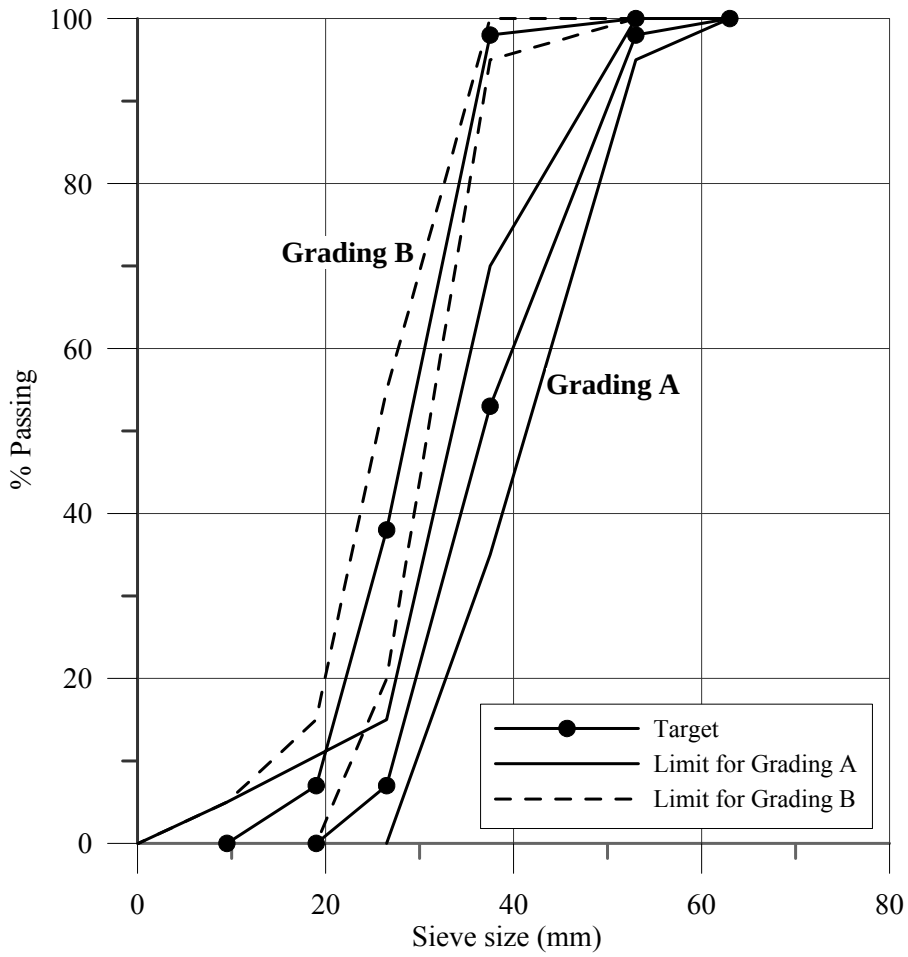

Note: Grading A: Used for concrete sleepers; Grading B: Used for steel sleepers

Figure 2.2 Particle size distribution envelopes of ballast material used in Queensland

Sub-ballast may or may not be present in rail track. In the absence of the sub-ballast layer, high maintenance efforts are likely as sub-ballast helps in protecting the upper surface of subgrade from the intrusion of ballast stones and acts as an inverted filter in the case of mud pumping while facilitating rainwater runoff and further distribution of loads. Suitable sub-ballast materials are broadly graded naturally occurring or processed sand-gravel mixtures, or broadly graded crushed natural aggregates or slag (Selig and Waters 2000).

Subgrade is the load-bearing layer of a track structure, either compacted natural ground or an imported fill embankment, which provides a permanent way to support the ballast layer. Subgrade soils are subjected to lower stresses than the ballast layer. The stress decreases with depth, and the controlling subgrade stress is usually at the top zone of the subgrade unless unusual conditions such as a layered subgrade of sharply varying water contents or densities may change the locations of the controlling stress. The soil investigation prior to design should check for these conditions. In some cases poor support is best avoided by changing the site or by removing unsuitable soil and replacing it with desirable soil or by chemical stabilisation (e.g. lime or cement).

2.1.1 Capping Layer

Capping layer (or an improvement layer) is a higher strength and higher stiffness layer introduced to protect weak natural ground or embankment fill by using a granular material. It serves as a temporary haul way which helps in solving the problem of subgrades wetting up and losing strength during construction by protecting the subgrades from the damage caused by site traffic. However, care and design must be undertaken not to instigate shear failure in both the capping layer and the subgrade. Practically it is not possible to build upon subgrades whose California Bearing Ratio (CBR) value is less than 3. It is, therefore,

necessary to improve the CBR value either by installation of a capping layer or stabilization of the natural ground or embankment fill.

Functions of capping layer are:

- to distribute loads over a sufficient area of the base preventing overstressing;
- to facilitate good drainage; and
- to prevent intrusion of ballast into subgrade.

The best material with which to construct a capping layer is a low plasticity well graded coarse-grained gravely material consisting of sand and gravel particles. It usually comprises of locally available low cost material such as crushed concrete, hardcore or poorly graded crushed rock, possibly with a binder included. In some instances a sub-ballast layer is also termed as a capping layer. In some railways, lime or cement stabilization of capping layer or subgrade is also common in practice.

QR uses capping layer design charts. These are based on CBR values, rail traffic loadings, maximum axle loads for the particular line, and operational parameters such as rail traffic, volume, speed and maintenance standards (Foun and Williams 2003). An example of a design chart for track with 22.5 tonne axle loads is shown in Fig. 2.3.

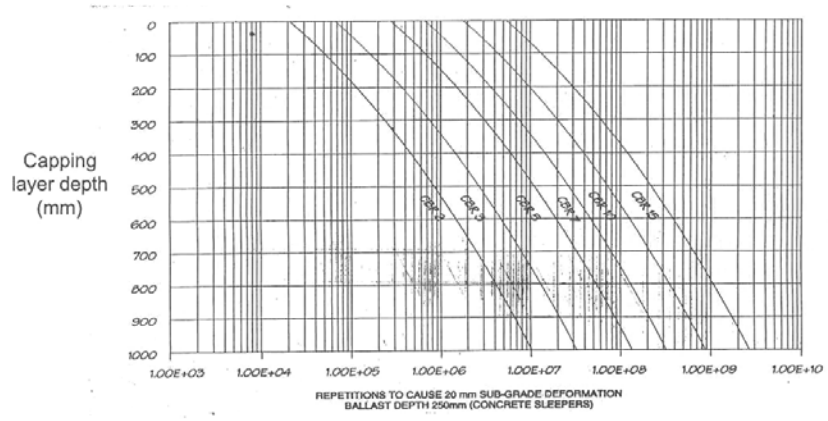

Figure 2.3 Capping layer design chart for 22.5 tonne axle loads (Foun and Williams 2003)

Subgrade failure usually occurs due to over-stressed conditions, poor construction or maintenance practices such as inadequate foundation preparation or inadequate compaction or excessive moisture content of the filling material. Similarly, natural conditions such as a weak subgrade soil (silt, clay), high groundwater tables and erosion or sliding of embankment also affect the performance of the subgrade. Therefore, it is essential that a sufficient crossfall between 1 in 20 and 1 in 40 is maintained on the upper surface of the subgrade to direct runoff from ballast towards a drain or cesspit to prevent water accumulation within the track structure. The subgrade is usually proof rolled to improve uniformity and reduce permeability and a proper drainage system will also accommodate the runoff from adjacent catchments as well as any ground water which could be present.

Although not wholly satisfactory, the main subgrade parameter commonly used in the design of railway tracks or road pavements is the CBR, which is an empirical measure of stiffness and the shear strength of the material tested. In the CBR test a standardised plunger of 50mm diameter is forced into the prepared soil specimen (contained in a rigid mould of approximately 150mm diameter and 200mm height) or in-situ ground and the load required to cause 2.5mm and/or 5mm penetration is measured. The penetration is standardised against the load required to cause the same penetration into a high quality crushed stone that is considered to have a CBR value of 100. The ratio of these loads is then used to calculate the CBR of the material.

$$\text{CBR}\% = \frac{\text{Load (or pressure) sustained by the specimen at 2.5 or 5.0mm penetration}}{\text{Load (or pressure) sustained by standard aggregates at the corresponding level}} \times 100$$

Australia Standards, AS1289.6.1.1-1998, AS1289.6.1.2-1998 and AS1289.6.1.3-1998 describe the method of measurement of CBR in laboratory and field. The CBR values are

then related to safe bearing pressures for different types of soil classification. Fig. 2.4 shows the approximate correlation of bearing capacity and CBR from Casagrande Chart.

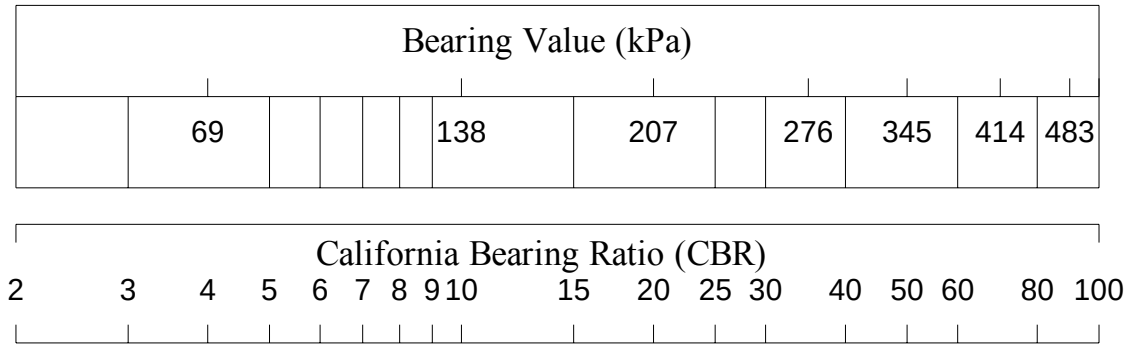

Figure 2.4 Approximate correlation of bearing capacity and CBR from Casagrande Chart (Jeffs and Tew 1991)

The soaked CBR is obtained by immersing specimens in water and allowing free access of water to the top and bottom of samples. The specimens are allowed to soak for 4days or the specified soaking period required. Soaked laboratory CBR values may not necessarily indicate the equilibrium situation or the stress history, but they do give an indication of the worst conditions of a soil. The natural soil moisture content after drainage is the correct moisture content for determining CBR values for railway designs. This is because during the course of time such natural soil conditions have been re-established. The drainage must be kept operating efficiently during the life of the rail track to prevent weakening of foundation due to loss of strength or decrease in CBR value due to rising water table. The use of CBR values is specified in the Railway Specifications for Earthworks (Queensland Rail - Civil Engineering Section 1998). For example, for new embankments a CBR of not less than 20 (soaked) is specified for capping layer materials. CBR tests on material with large aggregates can be very misleading if the resistance to the plunger penetration is provided by isolated larger particles. Similarly the only justification that a compacted clay

material be compared with crushed rock is that the test has a record of relative reliability and usefulness (Lay 1990)

To predict the gross behaviour of the track structure, a parameter known as the track modulus is used. Track modulus is a measure of stiffness of the gross track structure and is usually defined as the force per unit of deflection per unit of track length per rail. Zhang (2000) has indicated that the accuracy of track modulus evaluation is dependent on the theory and track models used. The properties of the subgrade are the dominant factors that influence the track modulus. The reason for this is that the influencing depth of subgrade is thicker relative to thin layers of ballast and sub-ballast. Selig and Waters (2000) state that the influence of traffic induced stresses extend downwards as much as 5m below the bottom of the sleepers. With low modulus, track substructure deflections will increase resulting in a decrease in riding quality as well as a significant increase in maintenance.

2.2 Track Degradation and Failure

2.2.1 Track Degradation

The development of irregularities of the top surface of rails or track alignment with increase in the number of load cycles is termed as track degradation. These irregularities lead to deterioration in riding quality. Track degradation parameters are usually measured by a track geometry-recording car, which detects rail level (top) variation, the curvature in horizontal alignment (versine), the difference in level of the rail (superelevation or cant), and the difference in cant over a given length (twist).

Of these track degradation parameters, twist is the most critical in terms of the risk of derailment. If a trailing axle of a wagon runs into a depression on the track, the diagonally opposite wheel is unloaded due to loss of contact with the rail as shown in Fig. 2.5. The danger in this phenomenon is that the lateral force acting on the wheels undergoing unloading of the vertical load may be sufficient to cause wagon derailment. Therefore, maintenance of the track geometry at specified standards is essential for a safe ride.

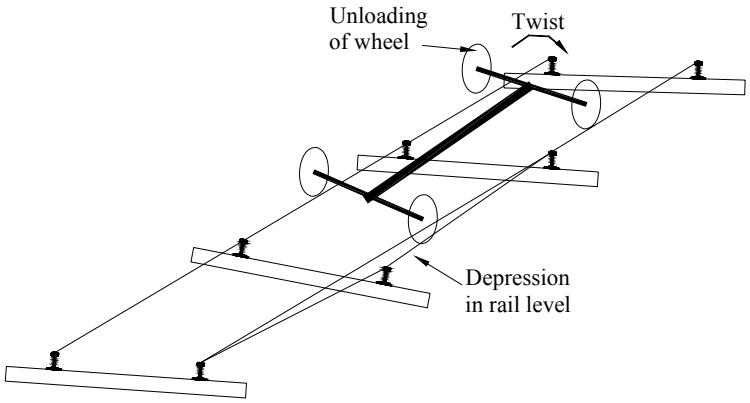

Figure 2.5 Effect of twist defect in track geometry

As per the discussion in Section 2.1, a key contributor to track degradation is the performance of the subgrade. This is due to the fact that natural ground properties can have a considerable variation within a few meters and are easily affected by seasonal moisture changes causing differential settlements. This phenomenon is aggravated by the repeated nature of the wheel passage or load cycle.

2.2.2 Subgrade Failure Modes

Fig. 2.6 shows a few factors that contribute to subgrade deterioration. The factors are repeated dynamic loading, excessive moisture and fine grained or poor quality soil. Selig and Waters, (2000) describe subgrade failure modes as follows:

- Excessive progressive settlement from repeated traffic loading;

- Consolidation settlement and massive shear failure under the combined weights of the train, track structure, and earth;
- Progressive shear failure from repeated wheel loading;
- Shrinking and swelling from moisture change;
- Frost heave and thaw softening; and
- Subgrade attrition.

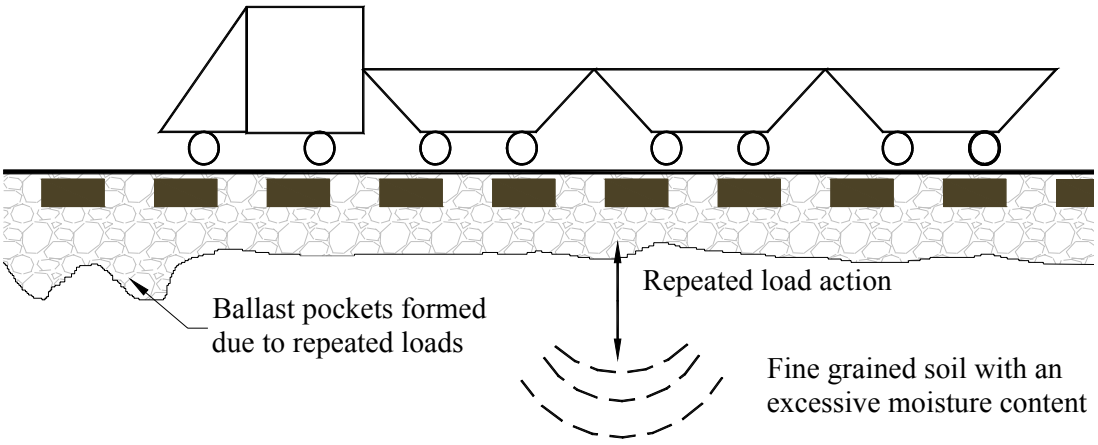

Figure 2.6 Subgrade deterioration factors

Firstly, the plastic flow of soil caused by excessive repeated loading at the subgrade/ballast interface leads to heave at the trackside through progressive shear failure (Fig. 2.7). This failure is prominent in subgrades of fine-grained soils with high clay contents. Secondly, non-uniform track settlement and unacceptable track geometry changes occur due to excessive plastic deformation caused by progressive soil compaction and consolidation.

Fig. 2.8 illustrates ballast pocket formation as a result of the vertical component of progressive shear deformation. This failure is caused by progressive compaction or consolidation of the entire subgrade layer because of repeated loading. Often this type of failure contributes to the development of non-uniform track settlement and unacceptable

track geometry changes. The other types of subgrade failures are subgrade attrition with mud pumping caused by high moisture content and repeated loading at the ballast and subgrade interface leading to ballast fouling and associated drainage problems, slope stability failures and excessive consolidation settlement due to self-weight.

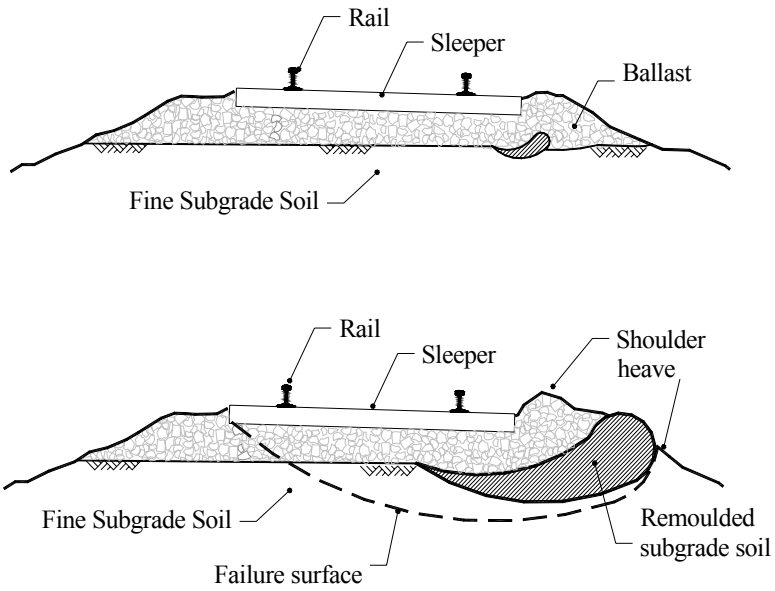

Figure 2.7 Subgrade progressive shear failure

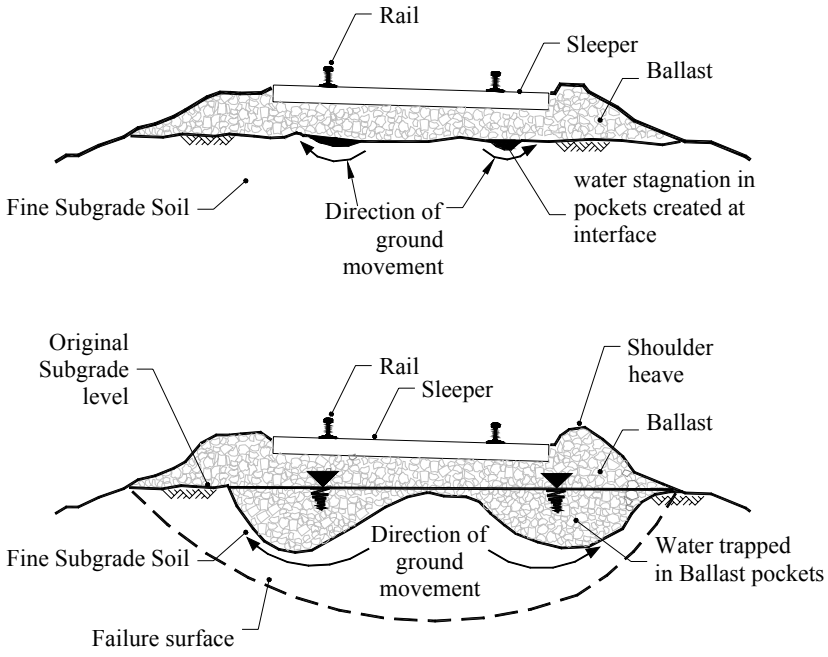

Figure 2.8 Ballast pocket formation

The most commonly used remedial measure, which is considered the most economical, is to increase the ballast thickness to reduce subgrade stresses. However, this method of remediation in association with excessive plastic deformation can also lead to formation of ballast pockets. The other possible remedial measures are constructing new track, increased rail weight, using a hot asphalt mix layer and modifying subgrade to permit higher stresses (Li and Selig 1998a; Li and Selig 1998b). These remedial measures adopted by the industry appear to provide only a short term solution by only treating the symptoms of the problems rather than analysing its root cause for longer term eradication. This thesis is an attempt to provide assistance towards developing a long lasting solution.

2.3 Response of Subgrade Layer to Rail Traffic

2.3.1 Mechanics of Load Transfer into Subgrade Layer

To calculate the vertical pressure on the subgrade layer resulting from sleeper loading, the load transfer through the ballast layer should be investigated. A comprehensive discussion of simplified theoretical models (Boussinesq elastic theory and stress below an evenly distributed strip load), semi-empirical (load spread methods and Schramm's solution) and empirical solutions (Talbot equation and Japanese National Railway equations) can be found in Jeffs and Tew (1991). Esveld (2001) has described the calculation of stresses based on Zimmermann's theory. The following gives a brief introduction to some of the above mentioned methods.

It is common in practice to analyse the rail track system for a static load, taking into account the dynamic effects of running speed on load by a Dynamic Amplification Factor

(DAF) also sometimes called the impact factor. The Eisenmann formula is the most recognised, based on track quality, and is given in Eq. (2.1) (Esveld 2001).

$$\text{DAF} = 1 + t\varphi \text{ if V} < 60 \text{ km/h}$$
$$\text{DAF} = 1 + t\varphi(1 + \frac{V - 60}{140}) \text{ if } 60 \le \text{V} \le 200 \text{ km/h} \quad (2.1)$$

where V = train speed km/h, φ = factor depending on track quality, and t = multiplication factor of standard deviation which depends on the confidence interval (Table 2.1).

Table 2.1 Values of t and φ (Esveld 2001)

Probability of occurrence in the field	t	Application
68.3%	1	Contact stress, subgrade
95.4%	2	Lateral load, ballast bed
99.7%	3	Rail stresses, fastenings, supports

Track condition	φ
Very Good	0.1
Good	0.2
Poor	0.3

Since the rail is so important for safety and reliability of rail traffic, a value of t = 3 is recommended as the chance of exceeding the maximum calculated stress is only ± 0.15%. On the other hand for subgrade stress calculation, a value of t =1 (corresponding to the chances of exceeding of ± 15.85%) is suggested.

Boussinesq elastic theory

This theory assumes that the ballast and the subgrade form a half space that is semi-finite, elastic and homogeneous and that the rail seat load is uniformly distributed over a circular area equivalent to the assumed contact area between the sleeper and the ballast.

$$\text{vertical stress} = P_a\left[1 - \frac{z^3}{(a^2 + z^2)^{1.5}}\right] \quad (2.2a)$$

$$\text{horizontal stress} = \frac{P_a}{2}\left[(1 - 2\nu) - \frac{2(1+\nu)z}{(a^2 + z^2)^{0.5}} + \frac{z^3}{(a^2 + z^2)^{1.5}}\right] \quad (2.2b)$$

where P_a = average uniform pressure over the loaded area (kPa), a = radius of the loaded area (m), ν = Poisson's ratio, z = vertical depth to any point beneath the surface.

Zimmermann's theory based stress calculation

The maximum vertical stress on the formation is calculated by superimposing contributions from the adjacent sleepers, which is assumed as uniformly distributed over each sleeper surface (Esveld 2001). The magnitude of this stress beneath the various sleepers caused by effective wheel load Q is given by

$$\sigma_i = \sigma_{\max} \eta(x_i) \tag{2.3}$$

in which

$$\sigma_{\max} = \text{DAF}.\frac{Qa}{2LA_{sb}} \tag{2.4}$$

$$\eta(x_i) = e^{-x_i/L}\left[\cos\frac{x_i}{L} + \sin\frac{x_i}{L}\right] \quad x_i \geq 0 \tag{2.5}$$

where a = sleeper spacing (centre - to - centre distance), A_{sb} = contact area between sleeper and ballast bed for half sleeper, DAF = dynamic amplification factor, and L= characteristic length determined by $L = \sqrt[4]{4EI/k}$ where EI = bending stiffness of rail and k = modulus of subgrade reaction.

As adjacent sleepers cannot all be subjected to an unfavourable load at the same time, the value of factor t is taken as unity when calculating DAF. The vertical stress at any location (x,z) is given by

$$\sigma_z = \frac{\sigma_i}{\pi}\left[\alpha_1 - \alpha_2 - \frac{1}{2}(\sin 2\alpha_1 - \sin 2\alpha_2)\right] \tag{2.6}$$

where σ_i = average uniform contact pressure between the sleeper and the ballast (kPa) and α_1, α_2 = as depicted in Fig. 2.9. Fig. 2.10 shows the stress pattern on the ballast bed along the length of the track.

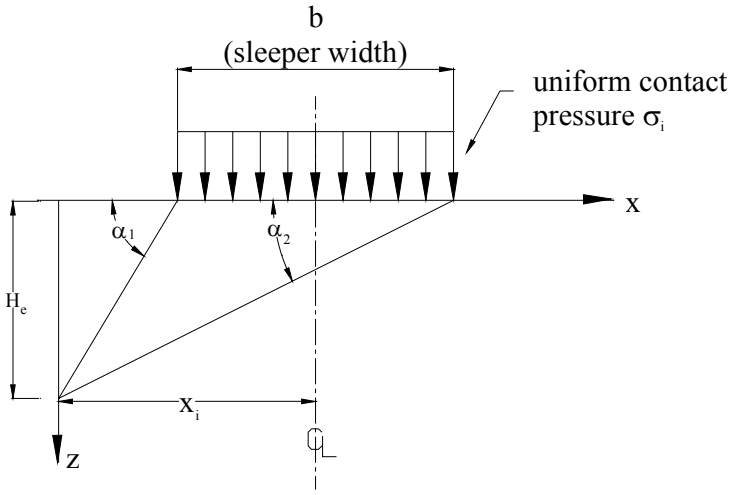

Figure 2.9 Stress due to strip load

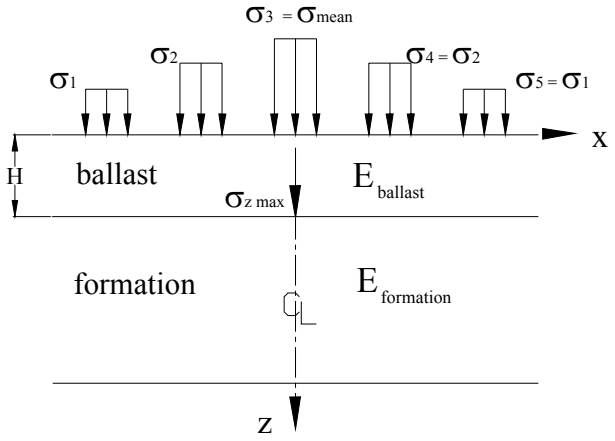

Figure 2.10 Ballast bed and formation represented as two-layer system (Esveld 2001)

In the Odemark's equivalence method, the two layered system is converted into a single layered system by

$$H_e = 0.9H \sqrt[3]{\frac{E_{ballast}}{E_{formation}}} \qquad (2.7)$$

where H_e = equivalent ballast depth, H = actual ballast depth under the sleeper, $E_{ballast}$ = modulus of elasticity of ballast, and $E_{formation}$ = modulus of elasticity of formation.

The maximum vertical stress on the formation in the actual two layered system then correlates with the maximum vertical stress in the equivalent half space at a distance H_e from the surface as shown in Fig. 2.9.

Load spread method

The assumption that vertical load is distributed vertically with a load spread slope of 1:1 or 2:1(vertical : horizontal) is the most commonly used simplified method in practice. Fig. 2.11 shows the mechanism of load transfer from the wheel to formation.

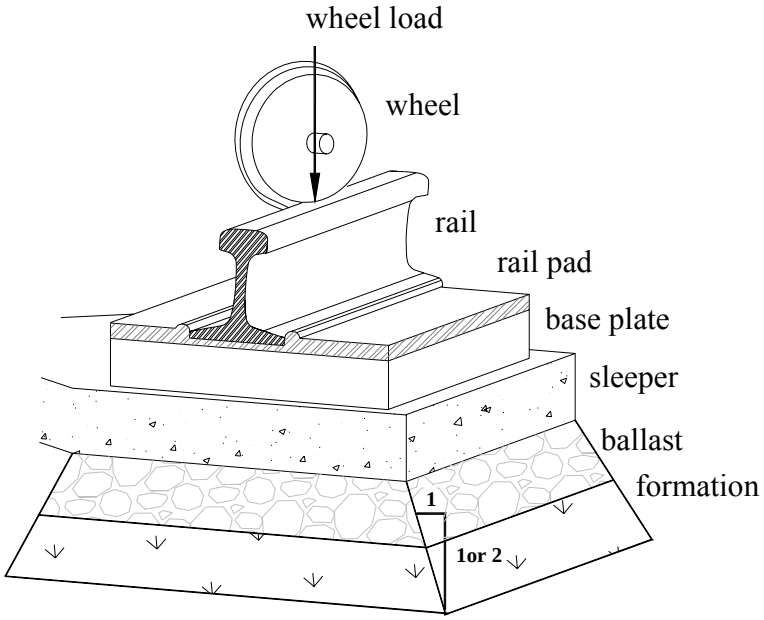

Figure 2.11 Load spread method

Jeffs and Tew (1991) indicated that the load spread method gives an average value of vertical stress at any given horizontal plane within the loaded area below the sleeper, while Boussinesq's method finds a maximum vertical stress. A comparison of these two methods (considering loaded area as circular) carried out by the Department of Industrial

Research, UK in 1991 is shown in Fig. 2.12. It was found that load spread of 2:1 is closer to Boussinesq than 1:1 load spread. The equations for 1:1 and 2:1 spreads can be derived in few steps as $\sigma_{average} = \frac{P_a}{\left[1+\frac{z}{a}\right]^2}$ and $\sigma_{average} = \frac{P_a}{\left[1+0.5\frac{z}{a}\right]^2}$ respectively.

Talbot Equation

The most commonly used empirical relationship to limit the subgrade stresses is the American Railway Engineering Association (AREA) recommended Talbot Equation developed in 1991. Li and Selig (1998a) have presented the Talbot equation shown in Eq. 2.8.

$$H = 0.24\left(\frac{P_m}{P_c}\right)^{0.8} \qquad (2.8)$$

where H = granular layer thickness (m), P_c = allowable subgrade pressure (138kPa recommended by AREA) and P_m = vertical stress applied on the ballast surface.

Li and Selig (1998a,1998b) identified the limitations of Eq. 2.8 as follows:

- Oversimplification of actual situation for tracks under heavier axle loads and higher train speeds;
- Not reflecting the effect of repeated dynamic loads on subgrade condition;
- Not considering the granular layer properties; and
- Assumption of a homogeneous half space that represents ballast, sub-ballast and subgrade layers without considering properties of individual layers.

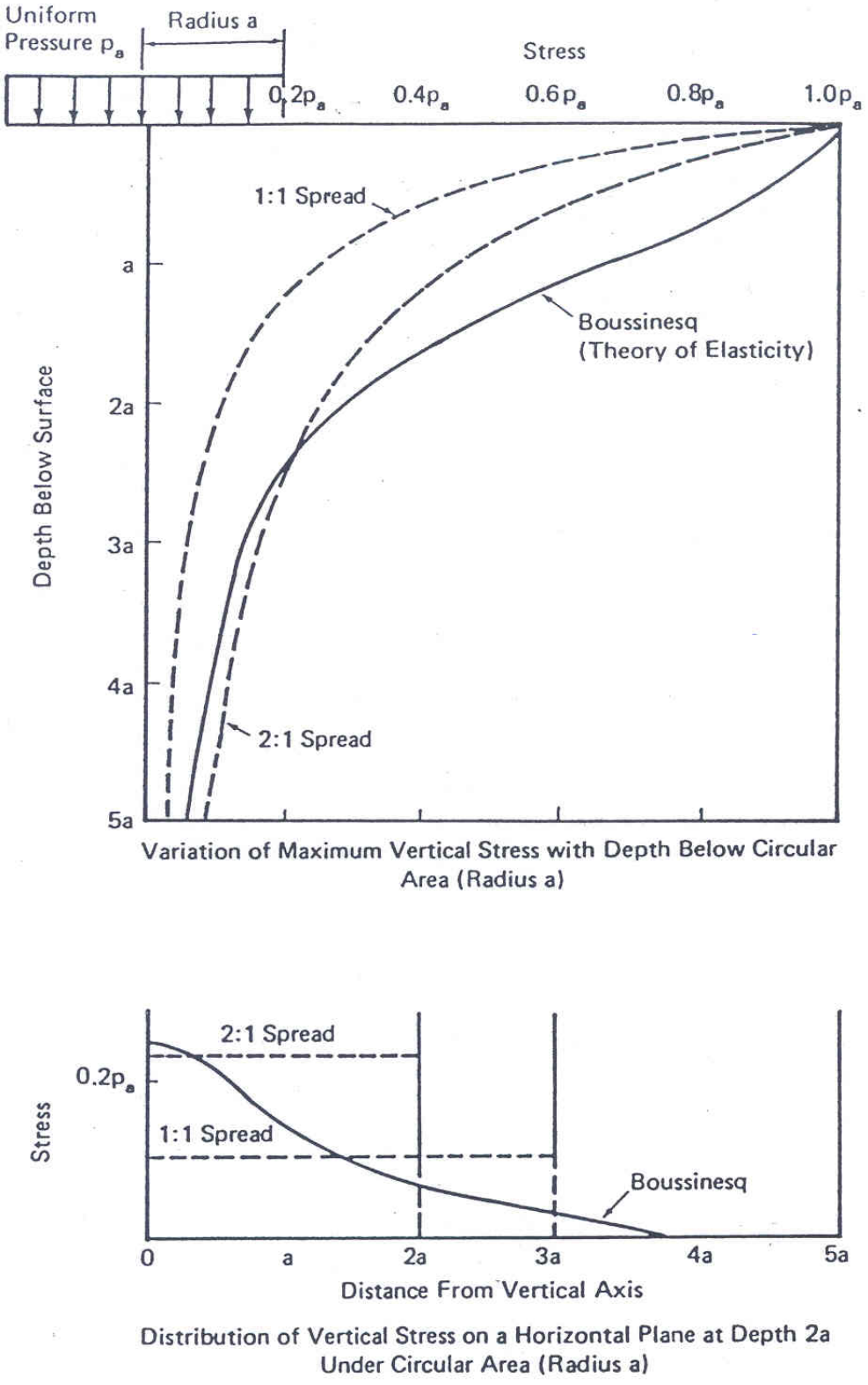

Figure 2.12 Comparison of vertical stress distribution under a uniformly loaded circular area by load spread methods and Boussinesq's equation (Jeffs and Tew 1991)

In fact all the methods described above have the limitations discussed by Li and Selig (1998a,1998b). Yet these methods provide simple, easy to use solutions in comparison with complex tedious multilayer theories or finite element techniques. Jeffs and Tew (1991) state that in 1968, Office of Research and Experiments (ORE) of the International Union of Railways (UIC) found the following important factors:

- The vertical stress distribution in the subgrade becomes practically uniform at a thickness of construction greater than 600mm.
- Sleeper spacing in the range 630 to 790mm had a negligible influence on the vertical stress level in the subgrade for a unit load applied to the sleeper.

2.3.1.1 Effect of Compaction and Moisture Content

Compaction is the process of increasing soil density or unit weight, accompanied by a decrease in air volume as shown in Fig. 2.13. There is usually no change in water content**.** The degree of compaction is measured by dry unit weight and depends on the water content and compactive effort (laboratory - weight of rammer, number of blows; field - weight of rollers, number of passes, frequency and amplitude of vibration).

The objective of compaction is to improve the engineering properties either of an existing soil or during the process of placing a fill. The main outcomes being sought are to:

- increase shear strength and therefore bearing capacity;
- decrease void ratio and therefore reduce future settlement and permeability;
- decrease swelling or shrinkage.

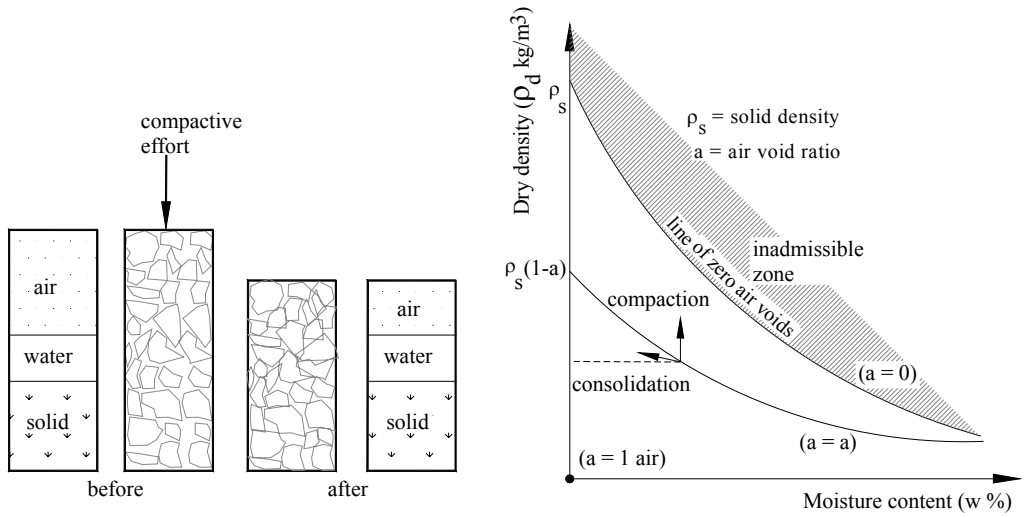

(a) material phases in soil (b) basic density, moisture content variation (Lay 1990)

Figure 2.13 Illustration of compaction

Fig. 2.14 shows that for a given compactive effort, there will be an Optimum Moisture Content (OMC) at which the dry density attains its maximum value. The higher the compactive effort, the lower will be the OMC and the higher will be the maximum dry density, which is the shift from curve b to curve c. Fig. 2.14 also shows how the effect of increased compactive effort will produce little increase in densification after a relevant stage until no further compaction is possible. Usually, reduction in densification at constant moisture occurs for equal incremental increases in compaction energy and it all stops as about 1% voids is approached.

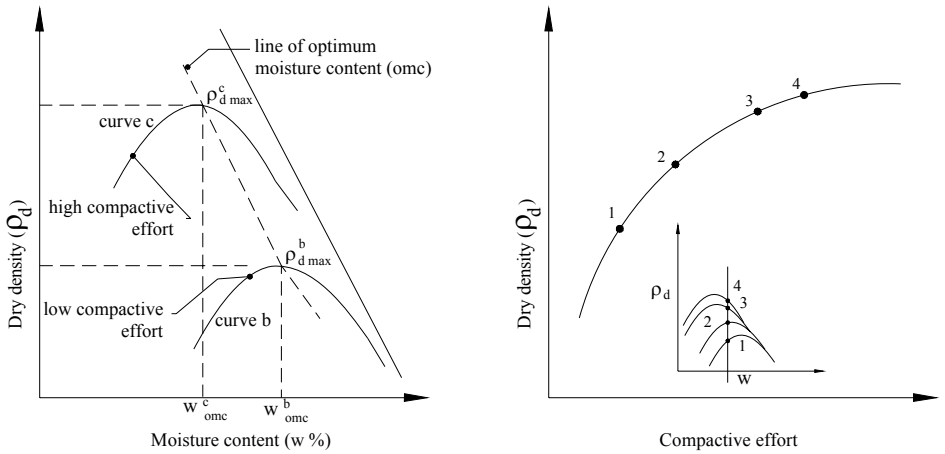

Figure 2.14 Effect of continued compactive effort (Lay 1990)

The increase in the moulding moisture content would results in a decrease in permeability on the dry side of OMC and a slight increase in permeability on the wet side of OMC. An increase in the compactive effort reduces the permeability and increases the dry density, thereby reducing the voids available for flow and increases the orientation of particles. Compaction rearranges soil particles and moves them closer together resulting generally an increase in the ratio of horizontal effective stress to vertical effective stress of soil (Lambe and Whitman 1979).

Well-graded coarse soils can be compacted to a high density compared to fine grained soils. OMC for fine grained soils is greater than that for coarse grained soils because finer particles have larger surface area and need more water to wet them. Thus for the same compactive effort, maximum dry density of fine grained soils will be less than that for coarse grained soils.

Fig. 2.15 shows the effect of three different densities on stress-strain characteristics curves obtained from consolidated undrained triaxial tests on sand specimens.

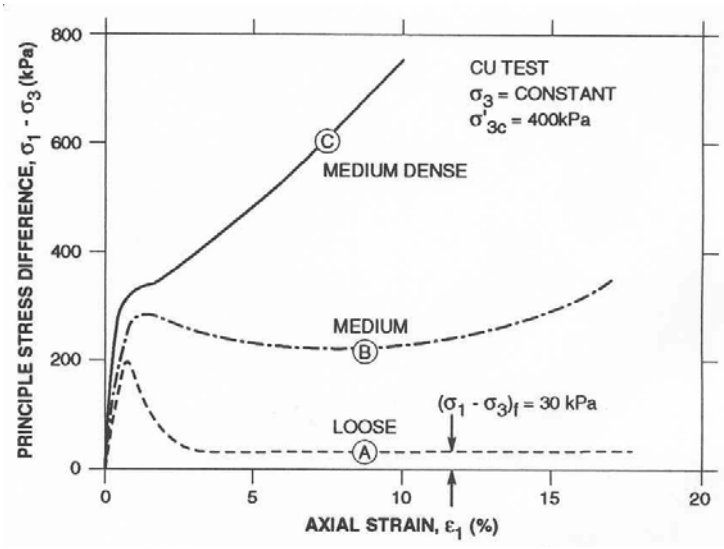

Figure 2.15 Effect of density on stress-strain behaviour of sand (Selig and Waters 2000)

Fig. 2.15 shows that there exists an increase in peak deviator stress with the increase in density for any given level of strain. This could be interpreted as indicating that, with an increase in density, the strength tends to increase due to closer packing of particles, increased friction angles and dilatency effects.

Natural subgrade moisture content is a direct function of seasonal fluctuations in the natural water table. Although the compacted moisture content is known at the time of construction, after a few years of service a substantial difference in moisture content is normally observed. Janssen and Dempsey (1981) explained the performance of subgrade due to different moisture conditions. Three major factors described by them are:

- shear strength (indicated by CBR) is inversely proportional to the moisture content (Fig. 2.16);
- dynamic and resilient modulus of unsaturated soils decreases with increased moisture content;
- frost heaving is influenced directly by already available water and indirectly by affecting the unsaturated hydraulic conductivity.

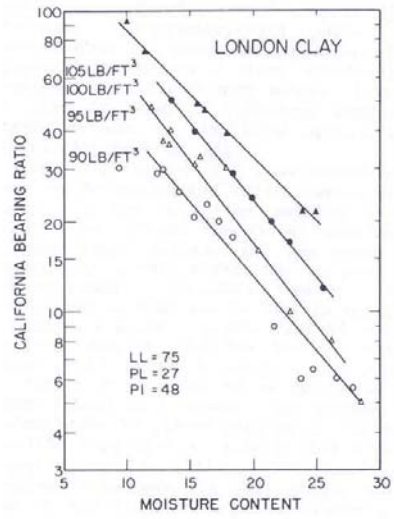

Figure 2.16 CBR vs. moisture content at various dry densities (Janssen and Dempsey 1981)

Ksaibati et. al. (2000) found that increasing moisture in subgrade and base layers of road pavements can significantly reduce the modulus values. The study was conducted using Dynaflect and Falling Weight Deflectometer (FWD) tests on Florida state roads, USA and the layer moduli were backcalculated. Table 2.2 tabulates their findings.

Table 2.2 Percentage of reduction in moduli due to moisture contents (Ksaibati et al. 2000)

State Road	Base			Subgrade		
	Range in moisture content (%)	Percent decrease in Dynaflect modulus	Percent decrease in FWD modulus	Range in moisture content (%)	Percent decrease in Dynaflect modulus	Percent decrease in FWD modulus
200	3.5	17.2	91.0	11	17.3	36.9
26	8.5	10.9	96.3	9.3	10.6	22.2
207	0.9	5.0	26.5	3.4	6.4	21.8
24	4.1	35.0	13.8	6.9	31.3	53.6
62	6.2	19.0	43.7	7.5	15.0	23.6

The effect of three different soil types (sand, silt and clay) on variation of compaction and stiffness achieved for increasing compactive effort are shown in Fig. 2.17. The percent compactive effort is the density expressed as a percent of maximum dry density in the ASTM standard compaction test. Effort is the work done by the compactor per unit volume of soil expressed as a percent of the effort in the ASTM test (Selig and Waters 2000). The main factors obtained from the excercise are:

- the coarser the material, the greater the percent compaction achieved;
- the finer the material, to achieve the same percent compaction requires greater compactive effort;
- the coarser the material, the greater the stiffness achieved due to compaction.

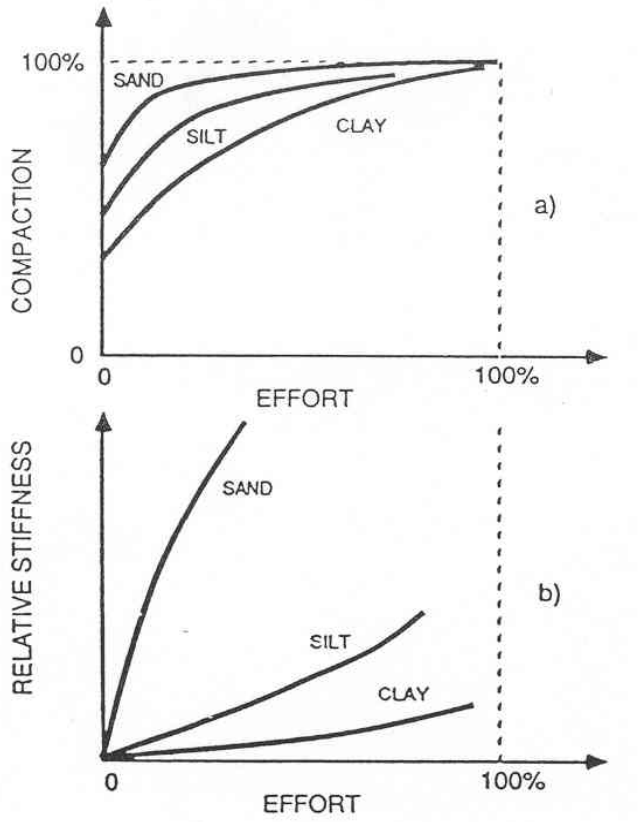

Figure 2.17 Effect of soil type on variation of percent compaction and soil stiffness with compaction effort (Selig and Waters 2000)

2.3.2 Effect of Loading Cycles

Means and Parcher (1964) discussed the effect of repeated loading, illustrating the typical stress-strain curves for initially identical specimens, one subjected to several thousands of repeated stress applications and the other in its initial compacted state before both being subjected to failure in a normal undrained test (Fig. 2.18), based on tests carried out by Seed and co-workers at the University of California on compacted clays. It was observed that the shear strength of clay increased due to a large number of repetitions of relatively low stress. However, if the stress intensities are too high, the cumulative deformation after a few repetitions will result in failure.

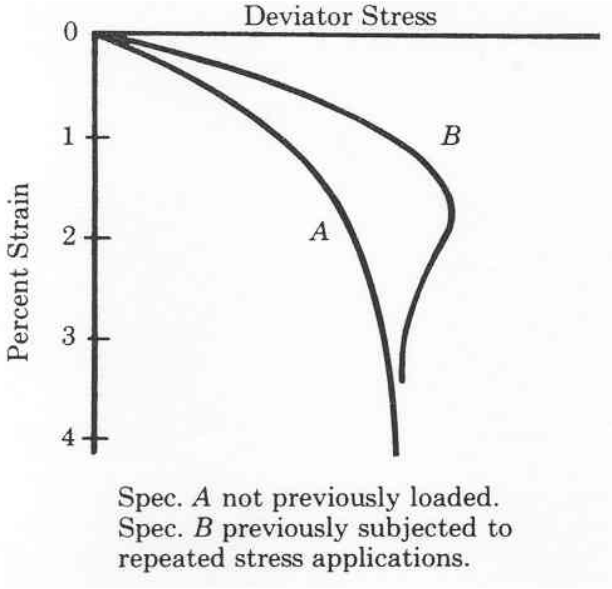

Figure 2.18 Effect of repeated loading (Means and Parcher 1964)

Fig. 2.19 illustrates the increase in constrained modulus during successive cycles of loading of Ottawa sand. The modulus is very sensitive to the early stages of loading, but this effect gradually decreases during successive loadings, stabilizing after several hundreds of cycles (Lambe and Whitman 1979).

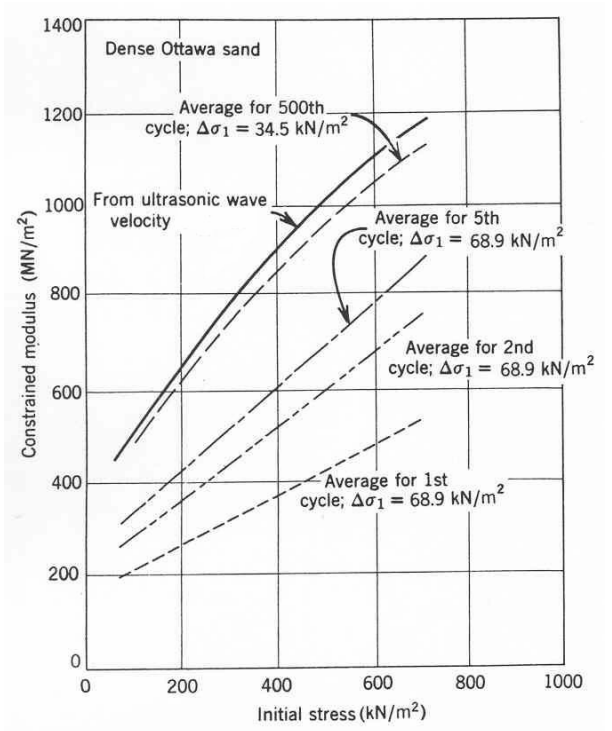

Figure 2.19 Increase in secant constrained modulus with successive cycles of loading (Lambe and Whitman 1979)

Fig. 2.20 shows stress strain behaviour of soil in oedometer test under repeated loading. At the first 10-50 cycles of a constant load application, a small amount of permanent strain is observed in sand which stabilized after several numbers of loading cycles (Fig. 2.20). As shown in Fig. 2.21, a sand sample becomes stiffer after the initial loading (Lambe and Whitman 1979).

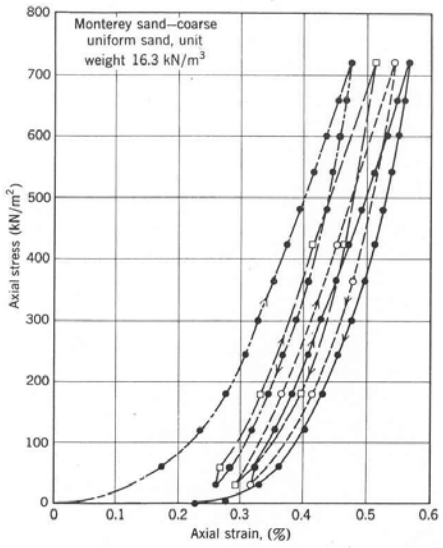

Figure 2.20 Stress strain curves for cyclic loading in oedometer test after Seamen et. al. 1963 (Lambe and Whitman 1979).

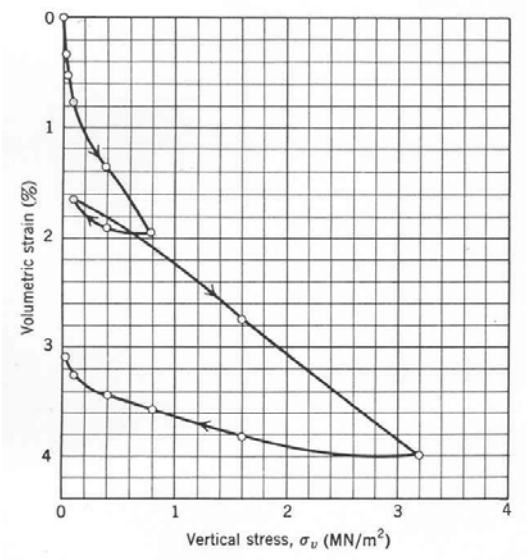

Figure 2.21 Oedometer test results for well graded calcareous sand from Libya (Lambe and Whitman 1979).

The stress strain characteristic of the railway substructure is dependent on the frequency and the size of the individual axle load applications. Profillidis (2000) has suggested that Dormon's rule, established in highway engineering, can be used for railways as well. Accordingly, the loading on the subgrade is inversely proportional to the number of loading cycles raised to a power λ, given by

$$\frac{\sigma_1}{\sigma_2} = \left(\frac{N_2}{N_1} \right)^{\lambda} \qquad (2.9)$$

where σ_1, σ_2 = stresses corresponding to N_1, N_2 loading cycles respectively and λ = an exponent with a mean value of 0.2.

If P = load per axle and T = daily traffic tonnage, from Eq. 2.9 it follows that

$$\frac{\sigma_1}{\sigma_2} = \left(\frac{T_2 / P_2}{T_1 / P_1} \right)^{\lambda} \qquad (2.10)$$

For constant axle loads, $P_1 = P_2$ and Eqn. 2.10 becomes

$$\frac{\sigma_1}{\sigma_2} = \left(\frac{T_2}{T_1} \right)^{\lambda} \qquad (2.11)$$

2.3.3 Stress-Strain Characteristics of Subgrade Layer

The appropriate measure of evaluating subgrade layer characteristics and its behaviour is dependent on its composition, structure, density and moisture content as well as the application. The material is usually tested for its performance under in-service conditions as much as possible. Behaviour of soils is very difficult to entirely match with simple elastic theory as they depart from it due to non-linearity, hysteresis and irreversible or plastic deformations when loaded as indicated in Fig. 2.22.

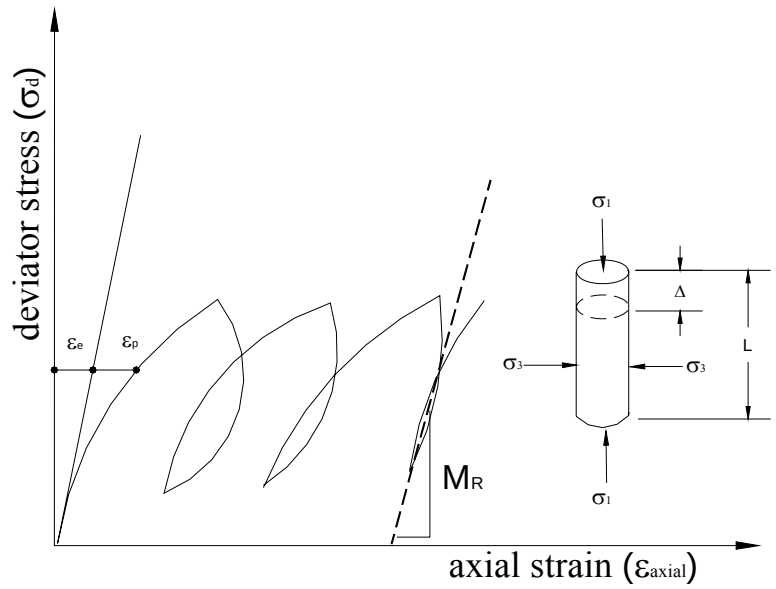

Figure 2.22 Stress-strain behaviour of soils

Fig. 2.22 shows the typical deviator stress and axial strain behaviour observed in a triaxial test, where a cylindrical soil sample is first consolidated to an isotropic stress and then subjected to an axial stress while holding the horizontal stress constant to cause shear failure. The axial stress is referred to as deviator stress. The axial deformation (Δ) on the original axial length (L) is also measured during the application of deviator stress. Thus, the vertical stress is the major principal stress (σ_1) and the minor (and intermediate) principal stress (σ_3) is the horizontal stress

The complex nature of the vertical, horizontal and shear stress patterns induced when a moving load approaches and departs a pavement is illustrated in Fig. 2.23. As shown an element in a pavement structure is subjected to positive vertical and horizontal stress components while the shear stress component is reversed as the load passes causing a rotation of the principal stress axes (σ_1) and (σ_3) (Lekarp et al. 2000).

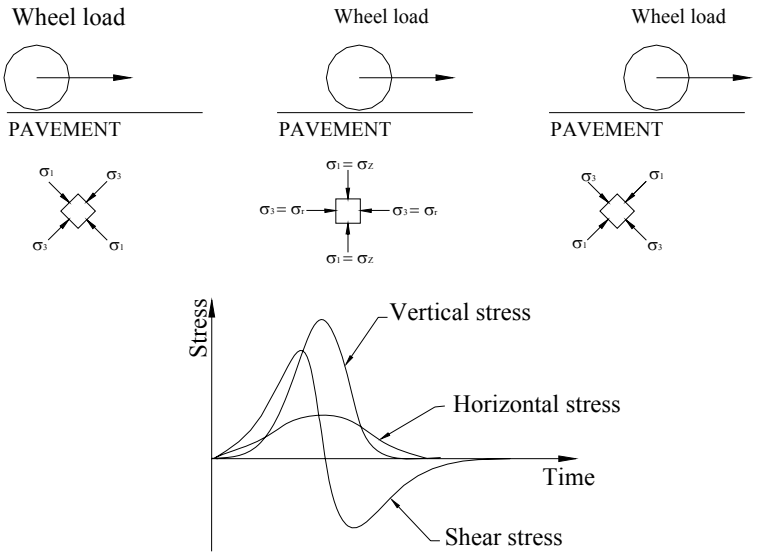

Figure 2.23 Stress beneath rolling wheel load (Lekarp et al. 2000)

Elastic behaviour

A soil is said to be elastic when it suffers a reduction in volume when a compressive load is applied but recovers its initial volume immediately when the load is removed. At the beginning of the stress-strain curve, soils present an approximate elastic behaviour since the strains are recoverable when the load is removed. Linear elasticity can be assumed if the loading is small enough to keep stresses and strains at low levels. The simplicity of this model has made it easy to produce closed-form solutions for many situations in engineering applications. The linear characteristics of a soil can generally be observed at very low strains in the order of 10^{-4} and smaller (Bowles 1979).

Resilient or recoverable behaviour

Resiliency is defined as the extreme limit to which a soil body can repeatedly be strained without fracture or permanent deformation. In the literature Resilient Modulus is considered as the most important property for both railway track and road pavement designs. It is defined as the rebound deformation from repeated load applications. *This is*

because permanent deformation is considered relatively insignificant to the resilient behaviour and is ignored in subgrade designs. As illustrated in Figure 2.22 the Resilient Modulus (M_R) is defined by the secant slope of the deviator stress (σ_d)-axial strain (ε_{axial}) curve given by:

$$M_R = \frac{\sigma_d}{\varepsilon_{axial}} \qquad (2.12)$$

where $\sigma_d = \sigma_1 - \sigma_3$ and $\varepsilon_{axial} = \frac{\Delta}{L}$ = axial strain in the direction of σ_1

σ_1 and σ_3 are the major and minor principal stresses.

Plastic or non-recoverable behaviour

Plasticity is defined as the ability of soil to undergo large deformations without crumbling or cracking under stresses. To define the permanent deformations, simple elasto-plastic models are generally used. As shown in Fig. 2.22, the stress-strain curve is represented by initial linear-elastic behaviour up to a yield stress, which limits the boundary between elastic and plastic domains. Once this yield stress is reached, plastic strains occur in addition to elastic strains. Usually the total strain is defined as the summation of these two strains:

$$\varepsilon = \varepsilon_e + \varepsilon_p \qquad (2.13)$$

where subscript $_e$ and $_p$ indicate, respectively, elastic and plastic strains.

Dynamic behaviour (Vucetic and Dobry 1991)

The dynamic behaviour of soils depends to a large extent on cyclic stress-strain characteristics of the soil in shear. Fig. 2.24 shows an idealised relationship between shear stress τ and shear strain γ for the first cycle of planar cyclic shear loading.

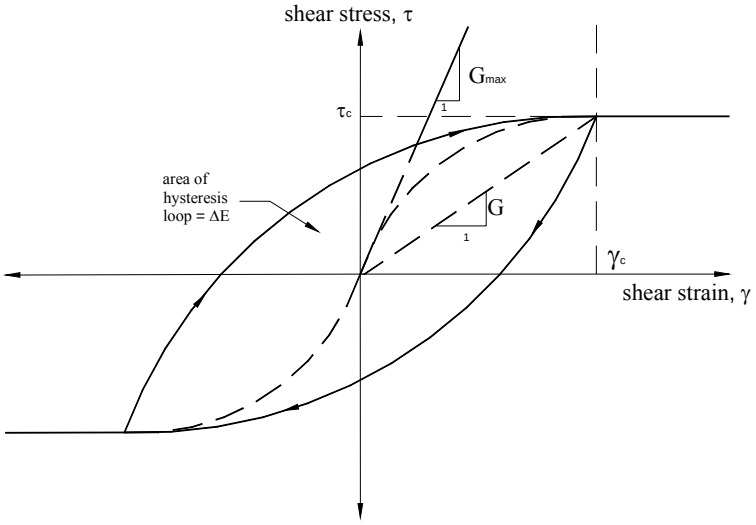

Figure 2.24 First cycle stress-strain curve

The dynamic characteristics are often described by:

a) Shear modulus at small strains, G_{max} given by

$$G_{max} = \rho V_s^2 \qquad (2.14)$$

where ρ = mass density of soil and V_s = shear wave velocity;

b) Secant shear modulus defined as

$$G = \tau_c / \gamma_c \qquad (2.15)$$

where γ_c = cyclic strain amplitude, and τ_c = cyclic stress amplitude corresponding to γ_c; and

c) Material damping ratio λ defining the progressive diminution of dynamic characteristics is given by

$$\lambda = \frac{1}{2\pi} \frac{\Delta E}{G\gamma_c^2} \qquad (2.16)$$

where ΔE = the area enclosed by the hysteresis loop as shown in Fig. 2.23.

Usually, G_{max} is obtained by in-situ seismic measurements of V_s and the influence of number of cycles, N on G is defined as the degradation of the modulus.

Most numerical models of railway track subgrade systems use elastic or elasto-plastic constitutive relationships (Section 2.5.2). Due to the large variability in the subgrade properties and the costs involved in testing, the practitioners experience considerable difficulty in establishing the appropriate resilient modulus for design purposes.

Subgrade moduli can be:

- determined from laboratory testing;
- backcalculated from nondestructive testing data; and
- predicted from soil/granular material properties.

Field/Laboratory Testing

There are basically two modes of testing available for the estimation of subgrade parameters, laboratory and field-testing. The most commonly used methods to determine subgrade material properties are repeated load triaxial tests, CBR tests, plate load tests, and unconfined compressive strength tests (Okada and Ghataora 2002). Table 2.3 lists the advantages and disadvantages of these methods.

Table 2.3 Merits and Demerits of the methods of measuring subgrade parameters (Okada and Ghataora 2002)

Test method	Type of result	Advantage	Disadvantage
Repeated load triaxial test	Secant modulus	Resilient modulus and shear strength can be measured	Time consuming
CBR test	CBR value	Widely used in highway pavement design	Closely related to shear stress
Plate load test	Elastic modulus	Related to CBR value	Slow to perform
Unconfined compression test	Compressive strength	Basic test	Measures static properties only

Nondestructive testing is also common in practice. The Falling Weight Deflectometer (FWD) test is generally used to backcalculate pavement moduli from field data, mostly in pavement design. This method has the advantage over other methods that it can be used to assess railway subgrade quickly without excavating the ballast. Most backcalculation procedures use a static pavement model to reproduce the deflection bowl generated from both static and dynamic surface deflection tests (Collop and Cebon, 1996).

In the case of fine-grained soils, an equivalent to in-situ CBR of subgrade can be assessed economically using the Dynamic Cone Penetrometer (DCP) test. In addition the Atterberg limits and particle size distribution (PSD) curves also are obtained. However, QR experiences show that when DCP is used, the resultant CBR that is estimated only represents the value at the tested fill moisture content. QR also uses ground penetration radar (GPR) tests to investigate the in-situ conditions (Foun and Williams 2003).

Laboratory Methods

Triaxial Test

Triaxial testing is the major laboratory testing for granular and subgrade materials. Elastic moduli, resilient moduli and permanent deformation behaviour can be quantified based on appropriate monotonic or repeated load testing data. A procedure for triaxial tests can be found in Australian Standards AS 1289.6.4.1-1998 and AS 1289.6.4.2-1998 for static load and AS 1289.6.8.1-1995 for repeated loads.

In the triaxial test, pneumatic, mechanical or electro-hydraulic repeated loading equipment is used to apply the required loading cycles (Brown et al. 1975). Computer controlled triaxial testing systems and software are also utilised (Menzies 1988). Specimen

deformation over the entire length, or in some cases, a portion of the specimen, is typically measured with either external or internal linear variable displacement transformers (LVDTs). Total, resilient and plastic deformations are typically recorded. Schematic illustrations of static and repeated load triaxial tests are shown in Fig. 2.25.

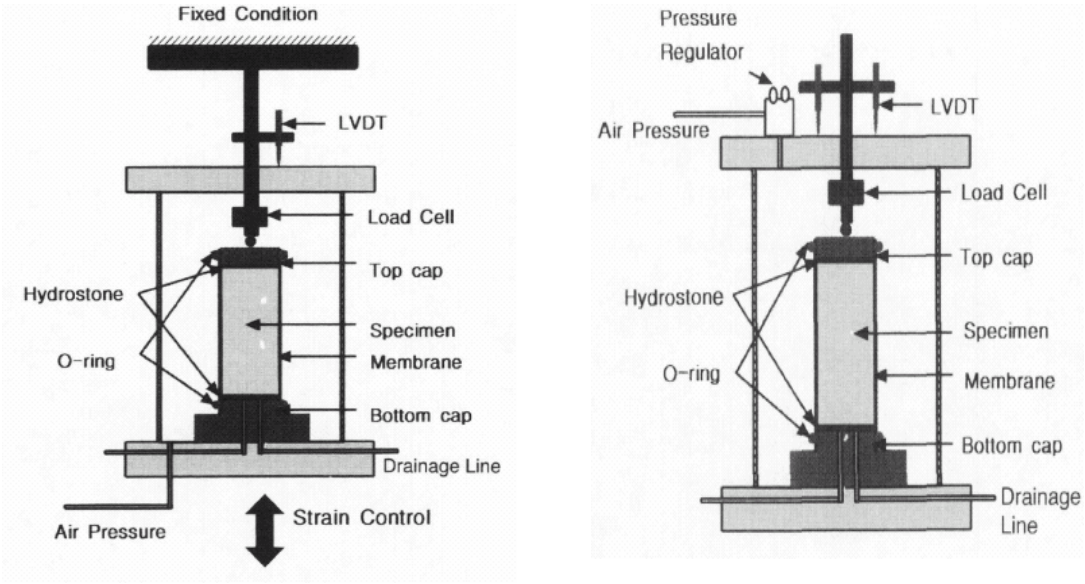

(a) static loading setup (b) cyclic loading setup

Figure 2.25 Schematic diagrams of the triaxial test setup (Kim et al. 2001a)

In drained triaxial tests, pore water is allowed to flow freely into and out of the soil specimen thus dissipating any excess pore pressure. In undrained triaxial tests, pore pressure is allowed to develop but there will be no flow of pore fluid. Fig. 2.26 shows typical stress-strain curves for triaxial compression of clays and sands.

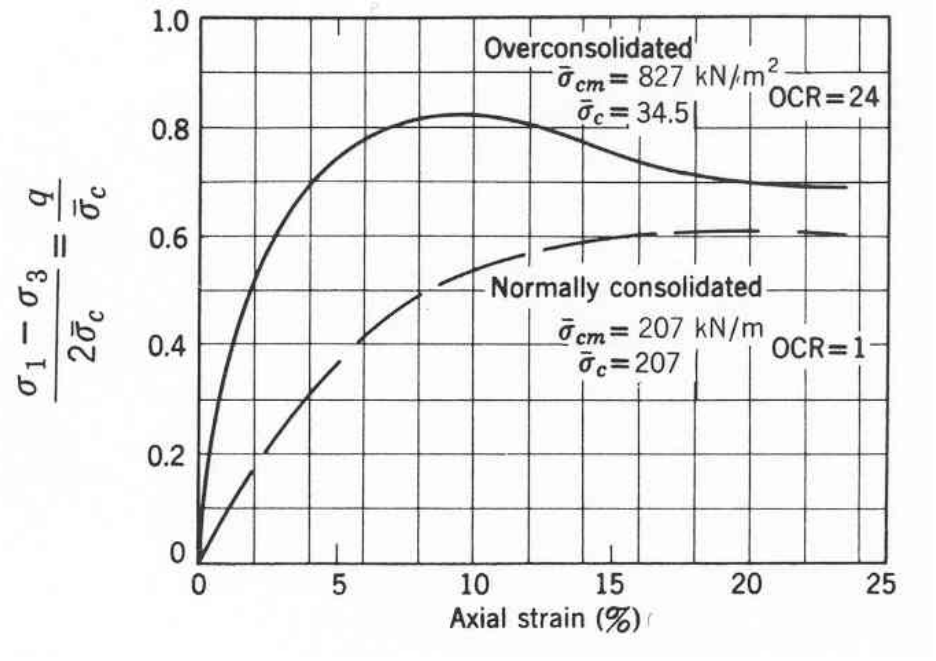

(a) Drained triaxial tests on Weald clay after Henkel, 1956

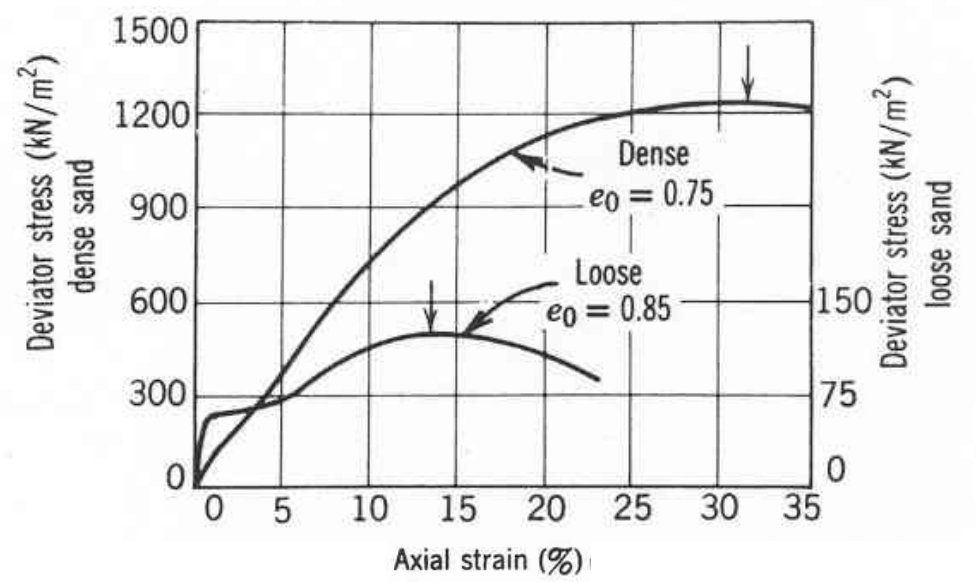

(b) Undrained triaxial tests on a saturated sand after Leonards, 1962

Figure 2.26 Stress-strain curves for clay and sand (Lambe and Whitman 1979)

Lambe and Witman (1979) have mentioned the following factors in their discussions on stress-strain behaviour of soils.

- Undrained strength behaviour of all soils is basically similar to that of clays;

- The effective stress-strain behaviour of granular soil is virtually the same for dry and saturated conditions;
- In granular soils, for normal stresses up to 14MPa the major contribution to the strain development is through the relative movement between adjacent particles and their rearrangement. A major cause of strain occurring above stresses of 14MPa is the crushing of granular particles;
- Dense sand and overconsolidated clays show similar stress-strain characteristics curves. The same similarity is observed in normally consolidated clays and loose sands;
- The stress-strain behaviour of clay is greatly dependent on the stress history of the sample. The higher the overconsolidation ratio, the stiffer the clay.

Field Methods

Dynamic Cone Penetrometer (DCP) Test

This method sets out the procedure for determining the resistance of soil to the penetration of a steel cone of 30 degrees angle and 20 ±0.2mm diameter driven with a 9 kg mass, dropping 510mm (AS 1289.6.3.2—1997). The DCP value is then related to CBR value through a known relationship that will vary for different materials and density. A discussion on various relationships is found in Harison (1989).

One such widely used relationship provided in Eqn. (2.17) is that proposed by Kleyn in 1975.

$$\text{Log } \mathbf{CBR} = 2.62 - 1.27 \log(\text{DCP}) \qquad (2.17)$$

where DCP = penetration mm/blow.

Nondestructive Methods

Falling Weight Deflectometer (FWD) Test

A method to determine the resilient moduli of the various in-situ flexible material layers and the subgrade soil, a nondestructive testing procedure called Falling Weight Deflectometer (FWD), is typically used for pavement evaluation for maintenance scheduling and overlay design. The FWD method measures the deflection basin or bowl (magnitude and curvature) under an impulse load derived from the kinetic energy of a free falling mass to simulate the effect of a moving wheel load. The surface deflection is measured from radially spaced velocity transducers. The moduli of the subgrade or pavement materials are then backcaluculated using these "measured deflection bowls". The principle is used to find a set of moduli to simulate the measured deflection basin through an error-minimisation procedure that locates the optimum solution. If the pavement material and subgrade soils to be encountered on a planned project are similar to those in an existing model then it is possible to utilise the backcalculated moduli in establishing reasonable and representative moduli inputs for a priori mechanistic design.

2.4 Material Models for Soils Subjected to Repeated Loading

2.4.1 Non-cohesive Soils

Models on resilient behaviour

Railway substructure materials characterisation generally includes resilient modulus. The resilient modulus of ballast (unbound granular material), and subgrade (fine grained soil) depends on the state of stresses within the track substructure. Over the years numerous models have been developed, especially in pavement design, which combine applied stress and material properties describing nonlinear stress strain relationships of soils and granular

materials under traffic loading. The following section gives a summary of material models currently available in pavement design, which in turn can be useful in proposing track substructure moduli.

The granular material models can be categorised as linear and nonlinear models. Shackel (1973) has described some of these models evolved based on resilient modulus as early as 1949. Accordingly, the model proposed by Terzaghi and Peck in 1949 is the earliest and the simplest linear stress strain model given by

$$E_t = K\sigma_3 \qquad (2.18)$$

where E_t = tangent modulus of cohesionless soil, K = constant, and σ_3 = confining stress. Shackel (1973) indicates that the model proposed by Biarez in 1962 is the earliest nonlinear model for cyclically stressed granular material given by

$$E_S = K\sigma_3^{\,n} \qquad (2.19)$$

where E_S = secant modulus, σ_3 = confining stress, and K,n = empirical constants.

Hjelmstad and Taciroglu (2000) indicate that the K-θ model of Hicks and Monismith (1971) has been a very popular material model since the late 1970's due to its simplicity. This model suggests that the resilient modulus is proportional to the mean compressive stress raised to a fractional power given by

$$M_R = K\theta^n \qquad (2.20)$$

where M_R = resilient modulus, $\theta = (\sigma_1 + \sigma_2 + \sigma_3)/3$ is the mean compressive stress (hydrostatic stress) acting on a sample in a triaxial test and K, n = empirical constants. σ_1, σ_2 and σ_3 are the major and minor principal stresses as defined in Figure 2.22. In a triaxial test the minor stresses, $\sigma_2 = \sigma_3$.

Hjelmstad and Taciroglu further indicated that Uzan (1985) has observed that the *K*-θ model did not comply with measured triaxial data and proposed a three-parameter model of the form

$$M_R = K\theta^n \sigma_d{}^m \qquad (2.21)$$

where $\sigma_d = (\sigma_1 - \sigma_3)$ and *K, n, m* = empirical constants..

In 1988, Witczak and Uzan generalized the model by Uzan (1985). They observed that σ_d coincides with the octahedral shear stress. The octahedral normal and shear stresses provide a better explanation for the stress state of a material in which normal and shear stress change during loading. This relationship is given in the following mathematical formulation

$$M_R(\theta, \tau) = K\theta^n \tau^m \qquad (2.22)$$

where θ, τ = octahedral normal and shear stress respectively, and *n ,m* = modal constants.

Thompson et. al. (1998) have carried out a comprehensive literature survey on granular material and soil moduli. Other than the above, several other modified models can be found in Thompson et. al. (1998) as follows.

Another approach adopted in predicting the resilient modulus of granular material is based on establishing a relationship to its volumetric and deviator strains (Thompson et al. 1998). The *K*-*G* model by Boyce (1980) described below is one such model.

Boyce (1980) model gives volumetric and deviator strains in the following forms

$$\varepsilon_V = \left(\frac{1}{K_i}\right) p^{\mu}\left[1-\beta\left(\frac{q}{p}\right)^2\right] \qquad (2.23)$$

$$\varepsilon_q = \left(\frac{1}{3G_i}\right) p^{\mu}\left(\frac{q}{p}\right) \qquad (2.24)$$

where K_i and G_i = initial values of bulk and shear moduli respectively, μ = constant less than 1, $\beta = (1-\mu)K_i/(6\ G_i)$, q = deviator stress and p = mean normal stress.

Statistical correlation between M_R and engineering index properties such as plasticity index, shrinkage index, etc. are useful in practice as basic engineering properties are easy and inexpensive to evaluate. However, the M_R values of granular material are neither related to the plasticity index nor to the conventional classification system. Some factors influencing M_R of granular materials are magnitude of the repeated stress state, gradation and moisture content, cohesion, friction angle, and static material strength properties (Tian et al. 1998).

Thompson et. al. (1998) after a thorough examination of their literature survey have concluded the following on granular material models:

- K-θ model is very simple but neglects the shear stress effect;
- Uzan model and its modifications consider both confining pressure and deviator stress effect; these models are shear stress related, and best for routine use giving reasonable results;
- Volumetric and shear strain related models are fundamentally sound yet complicated and more well suited for theory-related research than routine design use; and

- For a practical, accurate approach at least Uzan or one of its modifications should be employed in designs when characterizing granular material behaviour.

Models on plastic behaviour

The gradual accumulation of large numbers of small plastic deformations could lead either to failure or to stabilisation of a rail/pavement structure leading it to a fully resilient response. Insufficient research has been done to define reliable relationships between stress and plastic strain accumulation under repeated loading.

A comprehensive study on the permanent deformations of unbound granular material can be found in Lekarp and Dawson (1997, 1998) and Lekarp et. al. (2000). The modelling of permanent strain is done either considering the number of load applications or the stress conditions. The following summarises their findings:

- Barksdale (1972) has performed repeated load triaxial tests on different base course material with 10^5 load applications and suggested that the total permanent axial strain $(\varepsilon_{1,p})$ can be expressed by

$$\varepsilon_{1,p} = a + b\log(N) \qquad (2.25)$$

where N = number of load cycles, and a and b = constants for a given level of deviator stress and confining pressure.

- Sweere (1990) has observed that the above log-normal approach did not fit his results after 10^6 cycles and suggested a log-log approach given by

$$\varepsilon_{1,p} = aN^b \qquad (2.26)$$

where a and b are regression parameters.

- Wolff and Visser (1994) further investigated this log-log model for several million load applications and suggested

$$\varepsilon_{1,p} = (c\,N + a)\left(1 - e^{-bN}\right) \qquad (2.27)$$

where a, b and c are regression parameters.

- Paute et. al. (1993) have suggested a new approach to express the influence of number of load applications on the permanent deformations given by

$$\varepsilon^{*}_{1,p} = A\left(1 - \left(\frac{N}{100}\right)^{-B}\right) \qquad (2.28)$$

where $\varepsilon^{*}_{1,p}$ is the permanent strain after first 100 cycles, *A* and *B* are regression parameters.

- Lekarp and Dawson (1998) have suggested a relationship considering the maximum shear – normal stress ratio $(q/p)_{max}$, and the length of the stress path in p-q space applied to reach this maximum value given by

$$\frac{\varepsilon_{1,p}\left(N_{ref}\right)}{L / p_0} = a\left(\frac{q}{p}\right)^{b}_{\max} \qquad (2.29)$$

where $\varepsilon_{1,p}\left(N_{ref}\right)$ is the accumulated permanent axial strain after N_{ref} number of cycles, N_{ref} is any given number of load cycles greater than 100, *L* is the length of the stress path, a and b are regression parameters and p_0 is a reference stress introduced to ensure non-dimensionality of the equation.

Another approach found in pavement literature is the "shakedown theory" (Boulbibane et al. 2000; Collins and Boulbibane 2000; Raad et al. 1989; Sharp and Booker 1984). Shakedown is defined as the process of adaptation to the resilient (elastic) deformations after a certain number of cycles which stabilised permanent strains. If plastic deformations

do not stabilise, then some form of failure will occur. Lekarp and Dawson (1998) stated that the complex numerical models suggested in the literature treat this response of the whole pavement as a single unified structure. Lekarp and Dawson (2000) further state that the model predictions from Eq. (2.29) showed close similarities to the concept of shakedown theory.

2.4.2 Cohesive Soils

Models on resilient behaviour

Li and Selig (1994) categorise factors influencing magnitude of resilient modulus as:

- loading condition or stress state – magnitude of deviator stress and confining pressure, and the load cycles and their sequence;
- soil type and structure – depends on compaction method and compactive effort of a new subgrade; and
- soil physical state – moisture content and dry density which is subject to environmental changes.

Confining pressure was found to have less significant effect on resilient modulus than deviator stress for fine grained subgrade soils.

According to Thompston *et. al*. (1998) empirical models can be found related to soil strength such as the CBR value, and the following models are commonly used.

Model by Heukelom and Klomp, 1962;

$$M_R \text{ (MPa)} = 10 \text{ CBR} \qquad (2.30)$$

and the model by Lister and Powell, 1987.

$$M_R \text{ (MPa)} = 17.6 \text{ (CBR)}^{0.64} \qquad (2.31)$$

Typically, the cohesive soil materials are found to display a decrease in moduli with increasing amplitude of cyclic load, or increasing deviator stress as shown in Fig. 2.27. The nonlinear behaviour was defined in terms of the break point modulus and deviator stress as indicated in Fig. 2.27 and the intersection point was identified (σ_{Di}, E_{Ri}). The response, E_{Ri} was used in defining the subgrade properties and design algorithms (Drumm et al. 1990). These bilinear models are of the form given by

$$M_R = K_2 + K_3 (K_1 - \sigma_d) \quad \text{for } \sigma_d < K_1 \qquad (2.32a)$$

$$M_R = K_2 + K_4 (\sigma_d - K_1) \quad \text{for } \sigma_d > K_1 \qquad (2.32b)$$

where σ_d = deviator stress and K_1, K_2, K_3 and K_4 = modal parameters.

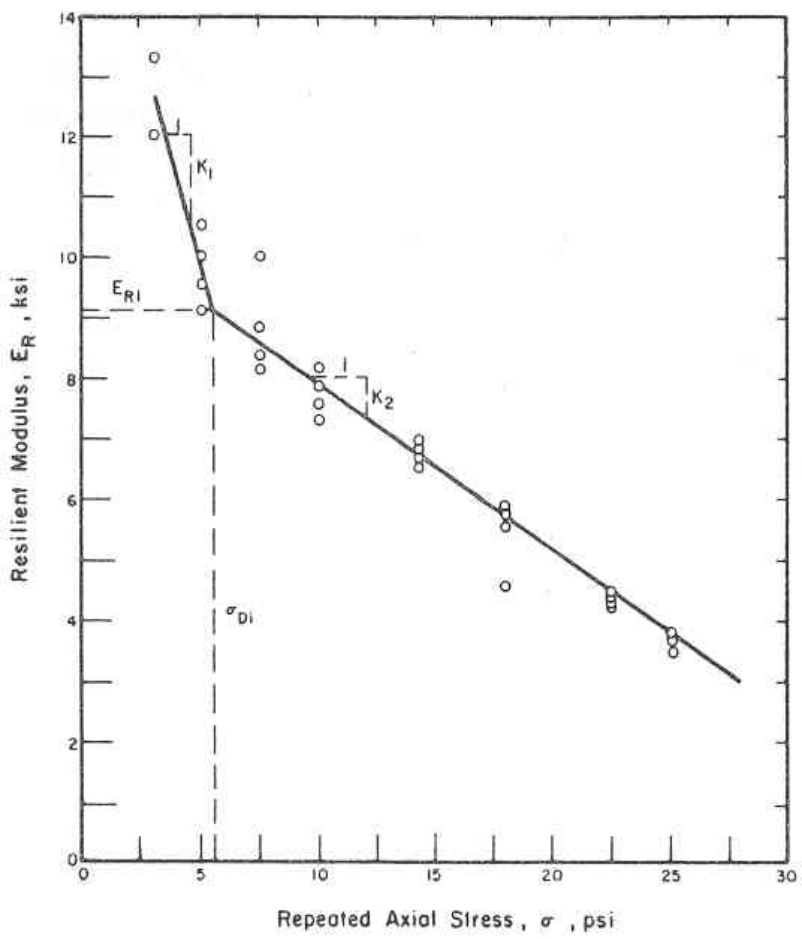

Figure 2.27. Typical variation in resilient modulus with deviator stress (Thompson and Robnett 1979)

Nonlinear models also are found in literature (Drumm et al. 1990; Li and Selig 1994; Thompson et al. 1998). These models are of the form

$$M_R = k\sigma_d^{\ n} \qquad (2.33)$$

where σ_d = deviator stress and k, n = modal parameters.

Drumm *et. al*. (1990) proposed a hyperbolic model. This relationship was arrived at by using the resilient response E_{Ri} proposed by Thompson and Robnett (1979) and correlating it to initial tangent modulus, unconfined compressive strength, plasticity index, dry unit weight, degree of saturation, and the percent passing #200 sieve. The model was given by

$$M_R = \frac{a + b\sigma_d}{\sigma_d} \qquad (2.34)$$

where σ_d = deviator stress and a, b = modal parameters.

Li and Selig (1994) summarised that bilinear, power, semilog, and hyperbolic models were able to fit the relationship between the resilient modulus and stress state for the soil tested by the respective researchers. They found that the best representations could be given in the order of bilinear, power, semilog and hyperbolic.

It was demonstrated in several studies that many factors influence the resilient behaviour of soils, plasticity index, moisture content, CBR value etc. (Drumm et al. 1997; Lee et al. 1997; Li and Selig 1994; Muhanna et al. 1999; Tian et al. 1998). The moisture sensitivity is one of the main factors addressed by the researchers. Li and Selig (1994) provide one such model considering moisture content and dry density

$$M_R = R_{m1} M_{R(opt)} \qquad (2.35)$$

where $R_{m1} = f_1(w - w_{opt})$, M_R = resilient modulus at moisture content w, and $M_{R(opt)}$ = resilient modulus at optimum moisture content w_{opt}.

Models on plastic behaviour

Three mechanisms are mainly responsible for the cumulative plastic deformation of fine grained soils. They are:

- Cumulative plastic shear strain;
- Cumulative consolidation; and
- Cumulative compaction.

The critical level of repeated deviator stress (often called the dynamic strength of soil) is defined as the stress above which the soil plastic deformation increases rapidly with cyclic loading. The dynamic strength of soil is usually smaller than the soil static strength determined under monotonic loading (Li and Selig 1996).

Puppala et. al. (1999) discussed a few of the models available in pavement literature for plastic strains in subsoils . They are:

- Lentz and Baladi (1981) model estimating the accumulated permanent strains (ε_p) of sandy soils which is similar to Equation (2.25) by Barksdale (1972)

  $$\varepsilon_p = a + b \ln N \qquad (2.36)$$

  where *a* and *b* are regression constants and N is the number of load repetitions.

- Thompson and Neumann (1993) have used a logarithmic permanent strain and a logarithmic load repetitions model expressed as:

  $$\log \varepsilon_p = a + b \log N \qquad (2.37)$$

  where a and b are modal constants. The term *a* varies and depends on the soil stress levels. The term *b* varies between 0.12 and 0.20 for the cohesive and granular soils respectively.

- Ullditz (1993) has developed the following plastic strain formulation recognising the limitations in earlier models:

$$\varepsilon_p = AN^{\alpha}\left[\frac{\sigma_z}{\sigma}\right]^{\beta} \qquad (2.38)$$

where σ_z = vertical effective stress, σ = reference stress that is equal to atmospheric pressure and A, α, β = constants.

- Puppala et. al . (1999) have modified the above model to accommodate the influence in confining pressure given by:

$$\varepsilon_p = AN^{\alpha}\left[\frac{\sigma_{oct}}{\sigma_{atm}}\right]^{\beta} \qquad (2.39)$$

where σ_{atm} = reference stress (atmospheric pressure of 100 kPa) and

$$\sigma_{oct} = \frac{\sigma_1 + \sigma_2 + \sigma_3}{3}$$

Li and Selig (1996) stated that the most common method used is the power model given by

$$\varepsilon_p = AN^b \qquad (2.40)$$

where A and b are parameters depending on soil type, soil properties and stress state.

To relate plastic deformations of cohesive soils in railway subgrades, Li and Selig (1998a) have suggested the following expressions:

$$\varepsilon_p = A\left(\frac{\sigma_d}{\sigma_s}\right)^m N^b \qquad (2.41a)$$

$$\rho = \int_0^T \varepsilon_p \qquad (2.41b)$$

where σ_d = soil deviator stress caused by train axle loads, σ_s = soil compressive strength, a,m,b =parameters depending on soil type, ρ = cumulative soil plastic deformation and

T = subgrade layer depth. Their design approach was to limit plastic strain and deformations for the design period.

2.4.3 Typical Subgrade Layer Materials

Subgrade materials also exhibit behaviour similar to other elasto-plastic materials where a yield locus could be defined. Beyond the yield locus significant plastic strains occur and within the locus plastic strains are relatively smaller and recoverable. Traditionally, in engineering practice, simplified and empirical approaches are adopted. Fig. 2.28 illustrates the behaviour of real soil showing complex hardening and softening behaviour.

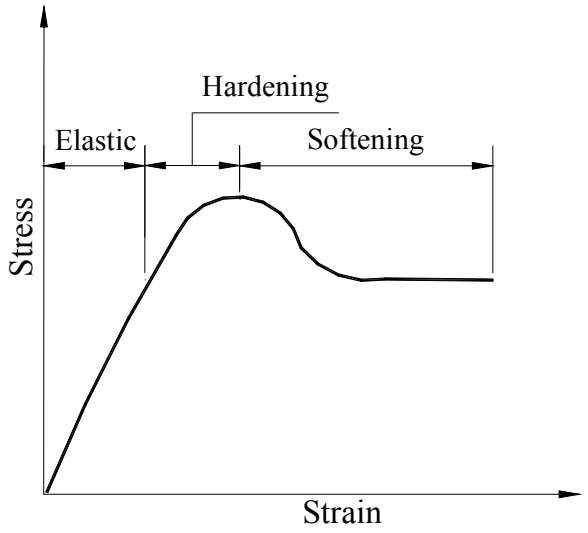

Figure 2.28. Real soil behaviour involving hardening and softening

There does not exist a single constitutive model which can describe the complex soil behaviour fully. The existing models have their own strengths and weaknesses according to the assumptions made to predict the behaviour of soils. The following briefly describes some of the constitutive models used in geotechnical designs. These models can be categorised as elastic and elasto-plastic models.

2.4.3.1 Elastic Models

The characteristic of an elastic model is that the direction of principal incremental stress and incremental strain coincides. These can be either linear or nonlinear models. The advantage of the elastic model is its simplicity. If one decides to explore beyond elasticity more complex numerical solutions on a computer are required.

Linear elastic model

Linear elastic model is based on Hooke's law. The loading and unloading moduli are kept the same in this model. There are four material parameters for an elastic model, elastic modulus (E), Poisson's ratio (ν), bulk modulus (K), and shear modulus (G) of which only two are independent.

K and G are specified as $K = E/3(1-2\nu)$ and $G = E/2(1+\nu)$.

Bilinear model

This model assumes that bulk and shear stiffness are constant until the stress state reaches the failure condition. The model requires two parameters to define pre-failure elastic behaviour and additional parameters to define failure surface. The pre-failure parameters required are either (E, ν) or (K, G). To define the failure surface parameters, for example, if the Mohr-Coulomb failure criterion is used, angle of friction (ϕ) and cohesion (c) are needed (Potts and Zdravkovic 1999).

Hyperbolic model

The hyperbolic model is defined by the following equation assuming a Poisson's ratio of 0.5

$$\sigma_d = (\sigma_1 - \sigma_3) = \frac{\varepsilon}{a + b\varepsilon} \qquad (2.42)$$

where σ_1 and σ_3 are the major and minor principal stresses, ε the axial strain and a and b are material constants as defined in Fig. 2.29.

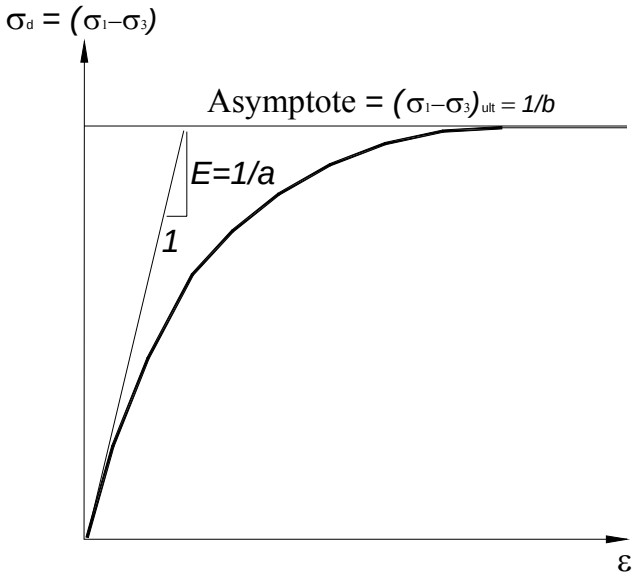

Figure 2.29 Hyperbolic stress-strain curve

2.4.3.2 Elasto-plastic Models

The elasto-plastic models assume that the material behaves in a linear elastic manner prior to yielding. The material behaviour after yielding can be defined as perfectly plastic, or strain hardening or strain softening plasticity. The fundamental difference between the behaviour of elastic and plastic models is that, in elastic behaviour the strain increments are proportional to stress increments (or linear), whereas in plastic behaviour strain increments are a function of the current stress state.

Some definitions associated with elasto-plastic models are given below.

Invariants

The six components for the stress vector (i.e., $\sigma_x, \sigma_y, \sigma_z, \tau_{xy}, \tau_{xz}, \tau_{yz}$) depend on the direction of coordinate axes selected. The principal stresses, generally denoted as $\sigma_1, \sigma_2,$ and σ_3, are invariant to the choice of axes. Therefore it is customary to use alternative invariants quantities in geotechnical designs. Some of the main invariants used as a combination of principal effective stresses are given below (Potts and Zdravkovic 1999).

Mean effective stress: $p' = \dfrac{(\sigma_1' + \sigma_2' + \sigma_3')}{3}$

Deviatoric stress: $J = \dfrac{1}{\sqrt{6}} \sqrt{(\sigma_1' - \sigma_2')^2 + (\sigma_2' - \sigma_3')^2 + (\sigma_3' - \sigma_1')^2}$

Lode's angle: $\theta = \tan^{-1}\left[\dfrac{1}{\sqrt{3}} \left(2\dfrac{(\sigma_2' - \sigma_3')}{(\sigma_1' - \sigma_3')} - 1 \right) \right]$

Flow rules

Plastic deformation depends on the stress state at which yielding of the soil occurs rather than on the route by which that stress state is reached. Yielding is associated with some plastic irrecoverable volumetric strain and some plastic shear strain. The relationship between plastic strain ratio and stress ratio is known as the flow rule governing the mechanism of plastic deformation or flow of the soil. If plastic potential and yield functions of a soil are assumed to be the same, the flow rule is said to be associated. When they differ, the flow rule is said to be non-associated. While there are many models describing plastic flow of materials, only a few models relevant to soils are described further.

Mohr-Coulomb model

The Mohr-Coulomb model is an elastic and perfectly plastic model with associated and non-associated flow rules. A hexagonal pyramid graphically illustrates this model and defines the yield surface (Fig. 2.30). Deformation prior to yielding is assumed to be linear elastic governed by the elastic parameters E and ν.

Yield function for the Mohr-Coulomb model in terms of stress invariants p', J and θ is given by:

$$f = J - \left(\frac{c'}{\tan \phi'} + p' \right) g(\theta) = 0 \qquad (2.43)$$

where $g(\theta) = \dfrac{\sin \phi'}{\cos \theta + \dfrac{\sin \theta \sin \phi'}{\sqrt{3}}}$, c' = cohesion, and ϕ' = angle of shearing resistance.

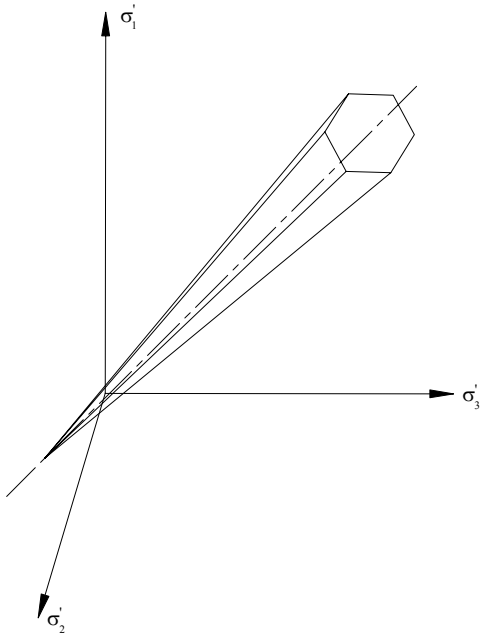

Figure 2.30 Mohr-Coulomb criterion

Drucker-Prager model

The Drucker-Prager model is an elasto-plastic model based on associated and non-associated flow rules. The yield surface is simplified to a cone in this model (Fig. 2.31).

Yield function for the Drucker-Prager model in terms of stress invariants p', J and θ is given by:

$$f = J - \left(\frac{c'}{\tan \phi'} + p' \right) M_{JP} = 0 \qquad (2.44)$$

where M_{JP} = constant independent of θ, c' = cohesion, and ϕ' = angle of shearing resistance.

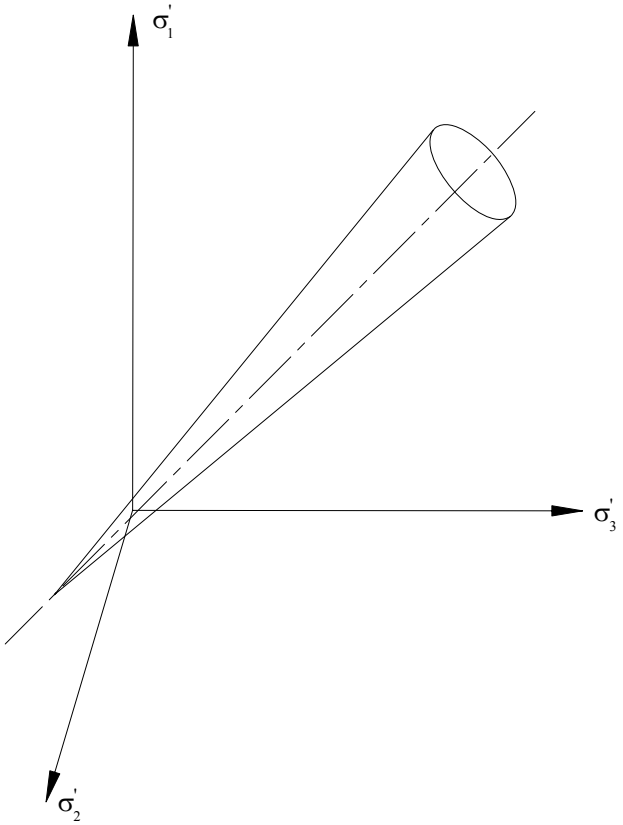

Figure 2.31 Drucker-Prager criterion

Critical state models

There are two critical state models, the modified cam clay model and the double yield surface model. The first is a time dependent model and the latter can be used as a time dependent or time independent model.

Modified cam clay model

The modified cam clay model is an elasto-plastic model with nonlinear elasticity prior to yielding. Elastic deformation is governed by bulk modulus and Poisson's ratio. The bulk modulus is related to the slope of the recompression line given by:

$$K = \frac{(1+e)p'}{\kappa} \qquad (2.45)$$

where e = current void ratio of the material and κ = slope of the recompression line in the plot of void ratio versus natural logarithm of p'.

The plastic deformation is defined by the yield function

$$f = \left(\frac{J}{p'M_J}\right)^2 - \left(\frac{p_0'}{p'} - 1\right) = 0 \qquad (2.46)$$

M_J = critical state parameter, and p'_0 = current isotropic consolidation stress.

Double yield surface model

This model employs the concept of double-yield criteria, which assumes that two yield surfaces are acting simultaneously. The total strain is decomposed into elastic (ε^e) and plastic (ε^p) components as in other models. In addition, the plastic component is subdivided into plastic strains associated with the two yield criteria given by:

$$\Delta\varepsilon = \Delta\varepsilon^e + \Delta\varepsilon^{p1} + \Delta\varepsilon^{p2} \qquad (2.47)$$

The elastic component is divided into time independent and time dependent components. Usually the time dependent component is related to creep and divided into distinct

interdependent volumetric and deviatoric components. The parameters for the model can be determined from triaxial and creep tests.

Constitutive models explore anything beyond elasticity and provide a rationale for the hardening and softening effects undergone by the subgrade material. These models are successfully adopted in a variety of commercially available computer programs.

2.5 Modelling of Railway Substructure

In the past, railway track substructure designs were based on empirical rules or on the beam on elastic foundation theory. With the availability of advanced computational power it is now possible to use advanced techniques such as the finite element methods. The following provides a brief overview of the existing methods.

2.5.1 Conventional Models

Simple elastic theory has been used to predict the mean maximum vertical stress in the subgrade with reasonable accuracy. The safe average bearing pressure (σ_{safe}) is defined as the ultimate subgrade bearing capacity (σ_{ult}) reduced by a factor of safety (x_L) $\leq$1.0. In designs this is used when the effect of settlement is considered negligible and the safety factor takes into account the plastic shear failure of the subgrade.

$$\sigma_{safe} = x_L \sigma_{ult} \qquad (2.48)$$

The most conservative estimate of bearing pressure is the allowable bearing pressure (σ_{des}), which takes into account both the settlement and shear failure. A settlement safety factor (x_s) $\leq$ 1.0 is introduced further reducing the safe bearing pressure.

$$\sigma_{des} = x_s \sigma_{safe} = x_s x_L \sigma_{ult} \qquad (2.49)$$

The design limits for the subgrade pressure determined by these methods are based on various static testing methods applied to saturated subgrades representing the worst possible subgrade condition. Jeffs and Tew (1991) further discuss the safety factors, indicating that Clarke (1957) has recommended that the settlement factor (x_s) be equal to 0.60. As a general rule, the maximum bearing pressure should not exceed about 83kPa for un-compacted formations and about 139kPa for compacted formations (Jeffs and Tew 1991). The 0.60 reduction factor is based on the AREA data, which accounts for the variability in sleeper support and track maintenance. Jeffs and Tew (1991) indicate that the AREA (1973) has recommended the calculations of allowable subgrade pressure be based on laboratory tests of saturated and remoulded samples (static triaxial tests).

To estimate the bearing pressure, the design (dynamic) wheel load should be doubled and the estimate be compared with the determined safe bearing pressure resulting in an equivalent settlement factor of 0.5. Table 2.4 illustrates the calculation of the design limit for subgrade pressure using both Clark and AREA settlement factors.

Table 2.4 Design limit bearing pressures of subgrades (Jeffs and Tew 1991)

Subgrade description	Average bearing	Design limit bearing pressure σ_{des} (kPa)

	pressure σ_{safe} (kPa)	Clark (1957) $x_s = 0.6$	AREA (1973) $x_s = 0.5$
Alluvial soil	< 70	< 42	< 35
Prepared ground not compacted	75-105	45-63	37-52
Soft clay, wet or loose sand	110-140	66-84	55-70
Dry clay, firm sand, sandy clay	145-210	87-126	72-105
Dry gravel soils	215-275	129-165	108-137
Compacted soils	> 280	> 165	> 140

Typical safe bearing capacities for compacted static loading of compacted subgrades have been well established in terms of a variety of testing techniques correlating the bearing capacity. The CBR test is considered as an adequate measure of safe bearing pressure of the subgrades.

The British Rail formation design method

British Rail has developed a "threshold stress" design method, limiting the stress on subgrade soils to protect against subgrade failure by excessive plastic deformation (Heath et al. 1972). The threshold stress was determined from repeated load tests on samples of London clay. The cumulative strain was measured as a function of loading cycles applied. Fig. 2.32 shows these results. The results have formed two distinct groups, one in which the deformation is progressive until complete failure and the other where the rate of deformation reduces to a stable condition.

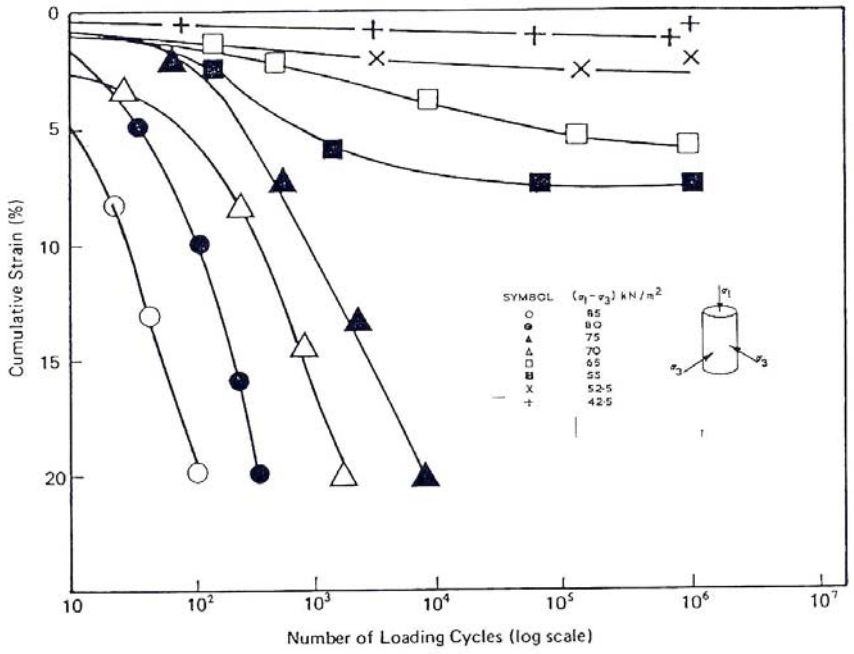

Figure 2.32 Cumulative strain resulting from repeated load tests of London clay (Heath et al. 1972)

Fig. 2.33 shows the modified strain-cycle (SN) relationships derived from repeated load tests on London clay. Here the failure number of cycles is defined at 10% cumulative strain, which is considered as a convenient limit failure (Heath et al. 1972). On this basis a limiting repeated elastic strain has been defined above which the deformation is continuous and below which it is terminating.

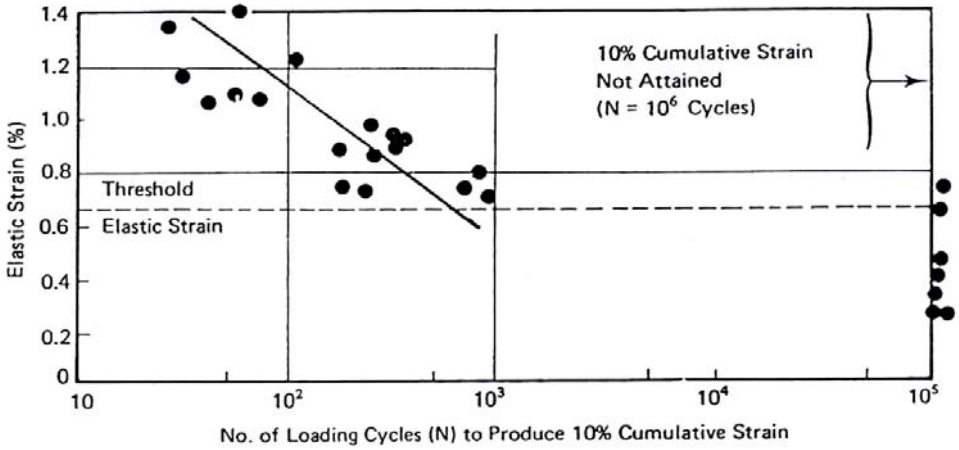

Figure 2.33 Modified SN curve (Heath et al. 1972)

Based on this definition, concept design charts have been developed by British Rail for selecting granular layer thickness for various subgrade soil conditions and axle loads (Fig. 2.34). The threshold stress/depth relationship is also superimposed on these curves, making it possible to determine the ballast depth required for a particular axle load induced threshold value. For example if an axle load of 79kN with a stress threshold of 60kPa is considered, then the required ballast depth would be about 425mm according to the chart. The limitations in applying this method are discussed by Raymond (1978) and Li and Selig (1998a,b). A summary of limitations is:

- Lumping of ballast, sub-ballast and subgrade as a single homogeneous layer neglects much higher stiffness of the top granular layer;
- The design often leads to a conservative granular layer thickness because of calculated stress levels in subgrade;
- This method uses a single value of axle load without considering cumulative tonnage i.e., the granular layer thickness will be the same for 10 million gross tons (MGT) or 100 MGT for the same maximum axle load; and
- The method is developed for clay and if used for gravel, sand, and low compressibility subgrades, the required granular depth is overestimated.

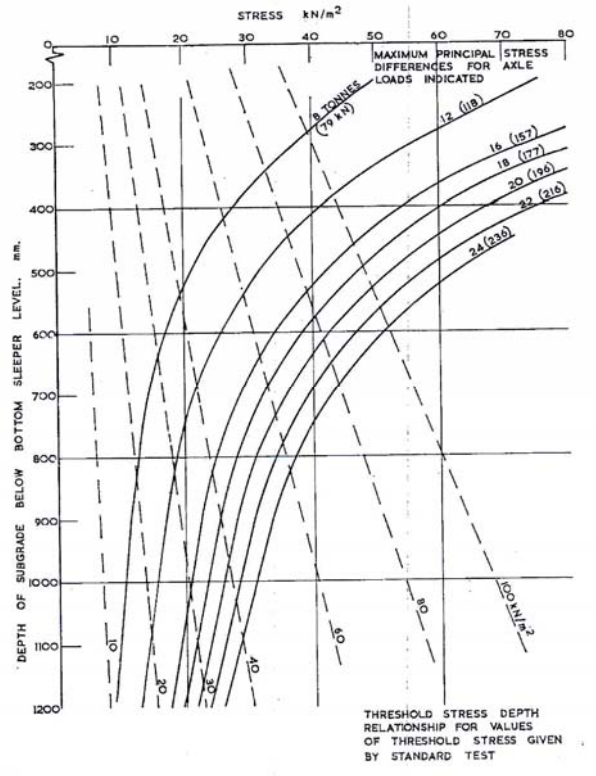

Figure 2.34 Relationship between induced stresses and soil strength (Heath et al. 1972)

German Railways empirical method

German Railways (DB) uses an empirical formula developed by Heukolom and Klomp in formation design. The permissible compressive stress σ_z on the formation related to number of loading cycles is given by:

$$\sigma_z = \frac{0.006E_{v2}}{1+0.7\log n} \qquad (2.50)$$

where E_{v2} = modulus of elasticity taken from the second load step in a plate load testing and n = number of load cycles.

Table 2.5 provides the permissible stresses according to Eq. (2.50) for two million cycles. The table also indicates the order of magnitude of the foundation modulus C when using a 300mm deep ballast bed with E=150MPa.

Table 2.5 Permissible stresses on formations (Esveld 2001)

Classification	E_{v2} (MPa)	C (N/mm^3)	σ_z (MPa) n=2x10^6
Poor	10	0.03	0.011
	20	0.04	0.022
Moderate	50	0.07	0.055
Good	80	0.09	0.089
	100	0.11	0.111

For the above formulation the DB standard demands an E_{v2} modulus of at least 120MPa just beneath the ballast bed. If the measured value from a plate load test does not comply with 120MPa, an intermediate layer is introduced. This intermediate layer in DB is a sub-ballast layer whose depth is determined according to Figure 2.35.

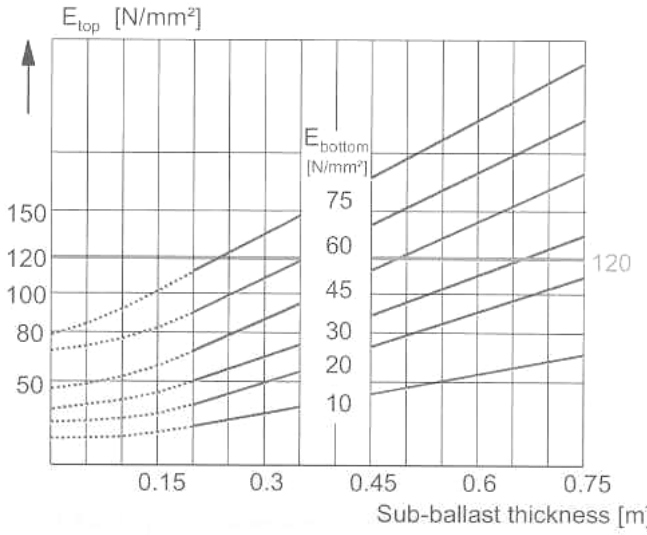

Figure 2.35 Thickness of sub-ballast layer according to DB (Esveld 2001)

According to this chart, if E_{top} = 100MPa & E_{bottom} = 60MPa, a sub-ballast depth of 0.25m is required. If E_{bottom} drops to 20MPa, the required sub-ballast depth is increased to 0.67m.

Beam on elastic foundation model

The beam on elastic foundation is based on the assumption that each rail acts like a continuous beam on an elastic support. The track foundation modulus, u is defined as the

supporting force per unit length of rail per unit vertical deflection of the rail as shown in Fig. 2.36.

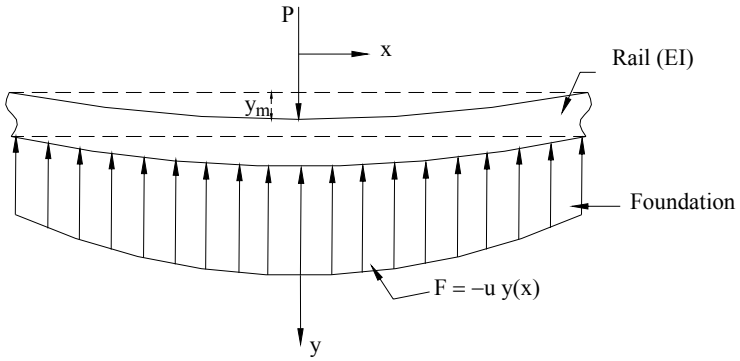

Figure 2.36 Beam on elastic foundation model (Selig and Waters 2000)

The rail foundation represents by u, includes the effect of fastener, sleeper, ballast, sub-ballast and subgrade. The track modulus cannot be calculated from the properties of each of these components and therefore the model is incapable of considering their individual effects. The differential equation of this model is given by:

$$EI\frac{d^4y}{dx^4} + uy = 0 \qquad (2.51)$$

where E = rail modulus of elasticity, I = rail moment of inertia, u = track foundation modulus x = any distance, x along the rail from the single point load P and y = rail deflection.

2.5.2 Numerical Models

As discussed previously, the conventional approaches disregard the effect of the constitutive material models on the behaviour of the track systems. It is advisable not to extrapolate the conventional models unless there is a sound basis on the fundamental approach to the problem. With the advent of numerical models, the analysis procedures have become more effective and reliable, incorporating complexities in geometry,

boundary conditions and material properties, but limited with the computer time and cost required.

The principles and concepts of numerical modelling methods can be found in many references, including Desai and Abel (1972), Smith and Griffiths (1988), Zienkiewicz and Taylor (2002) and an extensive list of references can be found in Desai and Siriwardane (1982). Dahlberg (2001) has summarised the mathematical models currently available in the literature, emphasising that track settlement is mostly considered as a function of loading cycles and/or function of the magnitude of the loading, but very little has been found in the literature on the material properties of track substructure. Following is a brief review of some of the existing numerical models.

Models on mechanical behaviour

The finite element models that consider mechanical behaviour of track and trackbed structure are discussed in this section. These models utilise failure criteria that consider the effects of static/repeated loading and material properties (modulus of elasticity, resilient modulus), but not the dynamic properties (dynamic shear modulus and damping).

Svec and Raymond (1976) developed a three-dimensional finite element model (CIGGT3D), which characterises the behaviour of ballast material stress path and its lack of ability to sustain tension, validated with full-scale model laboratory tests. The study thus concentrates on the effect of the sleeper and sleeper spacing on the contact pressure. Tayabji and Marshall (1977) presented a finite element structural model of conventional railway track support system (CRTSS). Here the finite element analysis was carried out in two stages, viz., a longitudinal analysis followed by a transverse analysis. The pseudo

plane strain technique was used in the analysis. Material non-linearity was accounted for by using the resilient modulus, and the load transfer was defined by two empirical parameters of sleeper-bearing length and angle of distribution.

Adegoke et. al. (1979) have studied three analytical models – MULTA, PSA, and ILLI-TRACK and evaluated their performance by comparing their predicted results with field measurements. The following is a brief description of each model.

MULTA - combines Burmister's three-dimensional elasticity solution with a structural analysis model that solves for the sleeper-ballast reaction. This model is restricted to homogeneous layers of linear elastic ballast and subgrade materials.

PSA – a finite element three-dimensional model with prismatic elements combined with a structural analysis model, which has the ability to incorporate property variations in both longitudinal and transverse directions. It is an expensive model compared to MULTA and ILLI-TRACK.

ILLI-TRACK – same model defined in CRTSS by Tayabji and Marshall (1977). The model has the ability to change material properties in the vertical, longitudinal and transverse direction. The limitations are the pseudo- three-dimensional assumption and the assumed model parameters, effective sleeper bearing length and angle of distortion. However it is the most cost effective method when considering computer cost and input-data preparation.

The three models were compared by Adegoke et. al. (1979) using constant moduli and Poisson's ratios. Figs. 2.37 and 2.38 show comparisons of the vertical pressure and displacement distribution under a single axle load. The results illustrate existence of some differences arising from the assumptions made in the distribution of load under the sleeper. This is reflected in the results of displacement as shown in Figure 2.38. However both MULTA and PSA models predict results of almost the same order while ILLI-TRACK predicts values in the order of 100 percent higher.

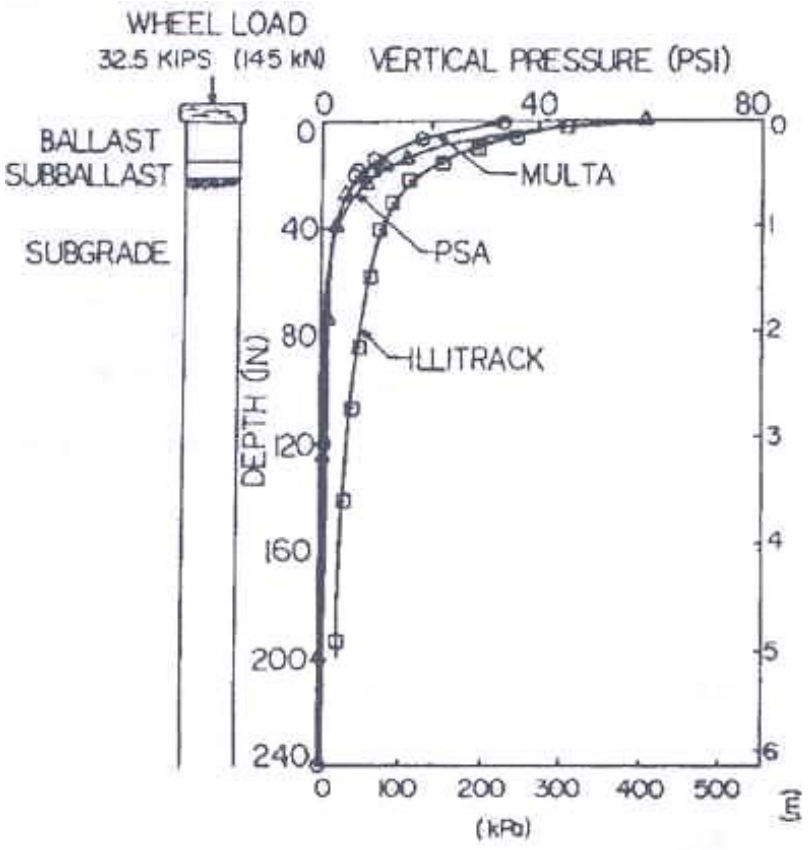

Figure 2.37 Comparison of distribution of vertical pressure with depth under single axle load: MULTA, PSA, and ILLI-TRACK (Adegoke et al. 1979)

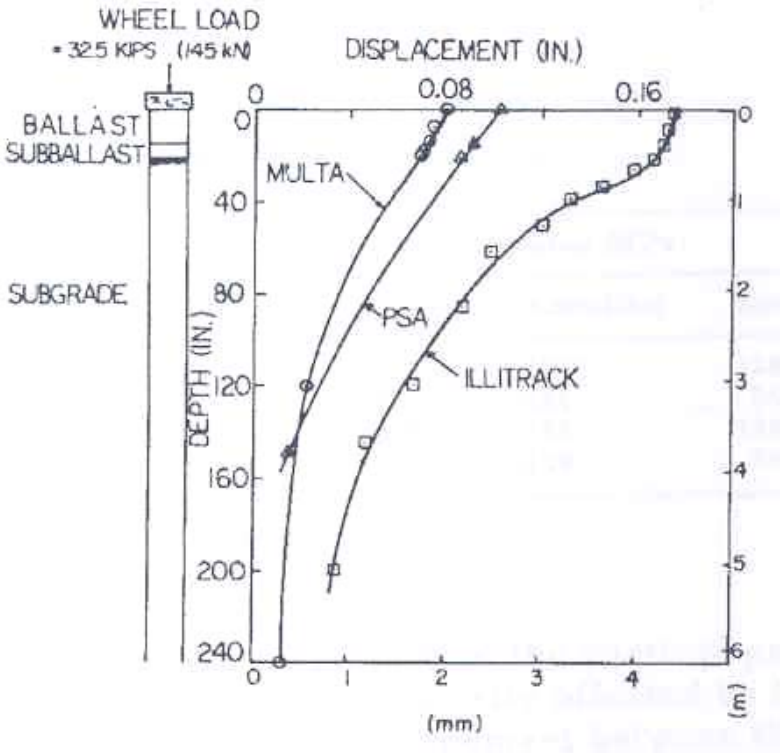

Figure 2.38 Comparison of distribution of vertical displacement with depth under single axle load: MULTA, PSA, and ILLI-TRACK (Adegoke et al. 1979)

The above observations were essentially the same as those obtained by Desai and Siriwardane (1982). The final conclusion reported by them is that irrespective of whether two- or three-dimensional analysis is used, proper care and judgement on factors such as the spacing and the length of the sleepers, and angle of load distribution is essential.

Chang et. al. (1980) have developed the GEOTRACK model – a three-dimensional multi-layer model considering the elastic response of the rail track system incorporating stress dependent material properties and separation of sleeper and ballast. Output of the model includes rail seat load, sleeper-ballast reactions, sleeper and rail deflections and bending moments.

Desai and Siriwardane (1982) developed several finite element formulations based on one-, two- and three-dimensional idealisation of rail track support system. The model procedures have been compared with results from ILLI-TRACK, MULTA and PSA models and with field observations. The main features of the models developed were:

- Provision of non linear elastic and elastic-plastic behaviour for model idealisations;
- Triaxial tests have been used to define model parameters;
- Use of special 'thin' interface elements between various components; and
- Use of special techniques to make computations as economical as possible.

Further, it was commented that though the one- and two-dimensional idealisations are possible in a number of situations, the non-linear three-dimensional analysis is the best to simulate practical problems; viz., loss of sleepers, local failures, sections near curves, fatigue failures due to repeated loading, etc.

Profillidis (1985, 1986) has presented a model to predict stress and strain at subgrade and sleeper and rail level. The method takes into account the different types of sleepers, the thickness of the track bed structure (ballast, sub-ballast and sand) and the quality of the soil of the subgrade.

Li and Selig (1998a,b) have presented a new design method for selecting granular layer thickness intended to prevent progressive shear failure and excessive plastic deformation due to repeated traffic loading developed based on the GEOTRACK model. Design charts have been developed covering various types of soils and granular layer conditions.

Models on Dynamic behaviour

The models that consider dynamic effects as a modelling parameter are discussed below. Here the models available on dynamic variation of loads or inclusion of damping coefficients are emphasised.

Zicha (1989) has developed a vibrating elastoplastic model of a high-speed track structure for the vertical and transverse load. In his discussion Zicha emphasised that with increasing velocity the vibrations penetrate to greater subgrade depths than usual and that subgrade has to be designed to withstand the special loadings induced by the dynamic phenomenon. The objective is to minimise plasticity and Zicha specifies a slightly more elastic subgrade material with careful drainage facilities and special transition zones between flexible and stiff foundations (eg. a tunnel or a rock cutting).

Cai and Raymond (1993) have presented a model incorporating rail and the sleepers as Timoshenko type beams, rail pads as linear springs with viscous damping and stiffness, and the vibration absorbing effect of track bed as a continuous array of linear springs and viscous dashpots. The study was done for a stationary vertical impact load.

Knothe and Wu (1998) have investigated a model that predicts vertical dynamic behaviour of a railway track on an elastic halfspace or on a layered halfspace.

Lei (2001) has developed a three-dimensional model in which rails, sleepers, fasteners and pads, ballast and track substructure are considered as a whole system. First, a wheelset model was used to derive the load spectrum varying with time. Then this load spectrum

was input into the three-dimensional model. Finally the dynamic response of the track structure was analysed under high-speed trains.

Sun (2002) has presented a closed-form solution of beam on viscoelastic subgrade subjected to a moving constant point load. The model has predicted that load velocities have significant effect on the shape of the dynamic deflection and the maximum deflection.

Models on Track response

Frohling (1997) formulated a model to predict differential track settlement due to dynamic wheel loading and spatially varying track support conditions. On-track measurements were used to analyse the model and mathematical simulations were used to predict future performance of the vehicle/track model.

Zhang (2000) has developed a model to predict track degradation. This model takes into account the degradation of each track component enabling prediction of either overall track condition or individual track component condition using various empirical relations approachs.

Shahu et. al. (1999) developed a three-dimensional linear elastic finite element model 3D20N to investigate the effect of track parameters on overall track response. The model was compared with other numerical models and field test data. Subgrade modulus was found to be the most influential track parameter on the overall track response. The parameters such as the depth of sub-ballast, rail moment of inertia, and sleeper spacing are also important.

2.5.3 Backcalculation Techniques

Backcalculation can be described as an inverse problem solution in which characteristics of material are assumed and adjusted until it computes the best fit to the measured deflection basin. Therefore, backcalculation can be defined as an error minimisation procedure. The analysis may be performed using iterations, database searching, closed-formed solutions or simultaneous equations. Usually the minimisation techniques employed use absolute or squared error with or without weight factors (May and Von Quintus 1994; Uzan 1994). Backcalculation analysis is very much sensitive to the assumptions made to interpret measured data in the mechanical model. For example most stress analyses carried out on pavement structures assume linear elastic response and uniform material properties. These assumptions lead to large errors in the best fit of the measured deflection basin and hence errors in the backcalculated moduli (Stolle 1990; Uzan 1994).

Further, the static response models used to reproduce the deflection bowls generated from static and dynamic surface deflection tests assume that the dynamic component of the response is unimportant. Instead these models assume that the deflection bowl is due to quasi-static response of the pavement (Collop and Cebon 1996). Collop and Cebon (1996) state that Tam and Brown (1989) examined the effect of simplification to quasi-static response and they concluded that the inertial effects are insignificant and a static model could be used with confidence in pavement analysis. They also concluded that material damping is a more important parameter than the inertia of the pavement.

In backcalculation, the real modulus or the damping coefficient or the components of the constitutive models used can be derived. The number of parameters is generally kept to a minimum so as not to produce instability in the set of equations to be solved (Uzan 1994).

Present pavement backcalculation models are based on multi-layered or two-layered systems. The moduli predicted from these models are sensitive to the input variables of the pavement such as layer thickness and the depth of bedrock (Uzan 1994). If two adjacent layers have relatively close moduli, it will be difficult to obtain realistic results using trial and error backcalculation methods since divergence or non-uniqueness is likely to render the iterative process ineffective (Shuo et al. 1998; Uzan 1994).

Most backcalculation procedures are developed for finding pavement layer moduli in highway and airport runway designs. Sussmann and Selig (2000) have used backcalculation techniques to find equivalent layer moduli of track layers using GEOTRACK. Elastic and plastic vertical deformations were measured by a multi-depth deflectometer installed to a maximum depth of 3m below top of sleeper. For the comparison of results, the correlated moduli of the cone penetration test (CPT) tip resistance and published results were used. These results were found to be favourable.

Backcalculation was performed in the current research to predict material properties using uniaxial compressive tests on soil samples in a rigid cylinder. The commercially available Finite Element program ABAQUS was used in predicting material properties. Details of this procedure can be found in Chapter 5.

2.6 Summary

Analysis and design of rail track substructure, in particular sub-ballast/capping layer has been reviewed in this Chapter. Effect of track degradation on the ride quality and

derailment potential has also been briefly described. Factors affecting degradation and failure of subgrade (natural ground or fill and capping layer) have been listed.
As the natural ground in subgrade is very complex with variable properties, attention has been focused on the capping layer analysis and design. For effective analysis of the capping layer, the stress level due to operational load is important. Various analytical, empirical and numerical methods used for the determination of stress levels in the capping layer are also provided and their advantages and disadvantages have been examined.

Effect of compaction, moisture content and load cycle on the physical characterisation has been described. Various tests methods used in the determination of the properties of the capping layer material have been provided. Various formulae used in the analysis of these experimental data have also been provided.

Basic theories of plasticity relevant to granular materials (soils) have been briefly presented. Various design methods of rail track substructure have been described in detail in the final section of this Chapter. The information provided in this Chapter will form the basic theory for the development of numerical modelling and experiments developed as part of this thesis.

The conventional track models are limited in their applications, as they do not address the performance of the substructure due to repeated application of axle loads, subgrade quality or ballast quality. Numerical models on the other hand incorporate all major components of track and subgrade (rails, sleepers, pads, ballast, subballast, and subgrade) yet lack proper characterisation of ballast and subgrade material properties, load distribution and the failure criteria chosen to develop the models. As discussed by Desai and Siriwardane

(1982) it is essential to use three-dimensional modelling in some cases to understand practical problems that occur in rail track structures; viz., loss of sleepers, local failures, sections near curves, fatigue failures due to repeated loading, etc.

The economic design and modelling of railway subgrade depends on proper characterisation of load deformation of materials. Resilient modulus has been identified as the concept to properly describe the behaviour of subgrade material subjected to repeated loading. Very few literature references were found on railway subgrade material moduli. However the literature on concepts and designs covered in pavements (highways and airfields) can be utilized for railway subgrades as well.

The most important factor affecting the resilient modulus of fine-grained materials was found to be the deviator stress, and this was identified to be most sensitive to the moisture content of the subgrade soil. As resilient modulus is sensitive to various soil indices, careful consideration must be given when utilising it in substructure analysis and design.

Granular materials display less variable characteristics compared to fine grained soils. Magnitude of repeated stress state, moisture content, degree of compaction and gradation are identified as significant factors influencing granular material resilient moduli.

Most researchers found that permanent deformation and log number of load applications were related in the form $\varepsilon_p = AN^b$. This equation is widely accepted in the practice of pavement design, especially for cohesive soils.

Static testing procedures are inadequate for characterising subgrade and granular material properties subjected to repeated loads. Repeated loading procedures are utilized to quantify the resilient modulus. Different testing procedures yield different M_R values and hence differences in substructure design.

Despite the sophisticated moduli obtained to represent the subgrade behaviour, CBR values and allowable subgrade bearing capacity form a larger content in design practices globally. Various charts related to CBR or allowable bearing capacities are readily available. This is common practice in railways and pavements design.

In characterising material properties, backcalculation techniques are used as a tool. The non-linear stress-strain properties are obtained by elastic layered theory in most of the backcalculation techniques used in pavement design. In the current research also, material properties are evaluated using finite element modelling based backcalculation techniques in which material properties are adjusted to best-fit the load-penetration response obtained from a semi-confined testing. This includes a series of small scale compressive tests. This laboratory study is presented in Chapter 3.